Role of C-terminal domain of *Mycobacterium tuberculosis* PE6 (Rv0335c) protein in host mitochondrial stress and macrophage apoptosis

Medha[1] · Priyanka[1] · Parul Bhatt[1] · Sadhna Sharma[1] · Monika Sharma[1]

Abstract

PE/PPE proteins of *Mycobacterium tuberculosis* (Mtb) target the host organelles to dictate the outcome of infection. This study investigated the significance of PE6/Rv0335c protein's unique C-terminal in causing host mitochondrial perturbations and apoptosis. *In-silico* analysis revealed that similar to eukaryotic apoptotic Bcl2 proteins, Rv0335c had disordered, hydrophobic C-terminal and two BH3-like motifs in which one was located at C-terminal. Also, Rv0335c's N terminal had mitochondrial targeting sequence. Since, C-terminal of Bcl2 proteins are crucial for mitochondria targeting and apoptosis; it became relevant to evaluate the role of Rv0335c's C-terminal domain in modulating host mitochondrial functions and apoptosis. To confirm this, *in-vitro* experiments were conducted with Rv0335c whole protein and Rv0335cΔCterm (C-terminal domain deleted Rv0335c) protein. Rv0335cΔCterm caused significant reduction in mitochondrial perturbations and Caspase-mediated apoptosis of THP1 macrophages in comparison to Rv0335c. However, the deletion of C-terminal domain didn't affect Rv0335c's ability to localize to mitochondria. Nine Ca^{2+} binding residues were predicted within Rv0335c and four of them were at the C-terminal. *In-vitro* studies confirmed that Rv0335c caused significant increase in intracellular calcium influx whereas Rv0335cΔCterm had insignificant effect on Ca^{2+} influx. Rv0335c has been reported to be a TLR4 agonist and, we observed a significant reduction in the expression of TLR4-HLA-DR-TNF-α in response to Rv0335cΔCterm protein also suggesting the role of Rv0335c's C-terminal domain in host–pathogen interaction. These findings indicate the possibility of Rv0335c as a molecular mimic of eukaryotic Bcl2 proteins which equips it to cause host mitochondrial perturbations and apoptosis that may facilitate pathogen persistence.

Keywords *Mycobacterium tuberculosis* · Rv0335c · Unique C-terminal domain · BH3-like motif · Mitochondria-mediated intrinsic apoptosis

Abbreviations

(TB)	Tuberculosis
(Mtb)	*Mycobacterium tuberculosis*
(TLR4)	Toll: like receptor 4
(MMP)	Mitochondrial membrane potential
(Cyt C)	Cytochrome c
(Ca^{2+})	Calcium

✉ Monika Sharma
monika.sharma@mirandahouse.ac.in

Medha
medha1.singh@mirandahouse.ac.in

Priyanka
priyanka.taank@mirandahouse.ac.in

Parul Bhatt
parul.bhatt@mirandahouse.ac.in

Sadhna Sharma
sadhna.sharma@mirandahouse.ac.in

1   DSKC Bio Discovery Lab And Department of Zoology, Miranda House, University of Delhi, Delhi 110007, India

Introduction

Mycobacterium tuberculosis (Mtb), the causative agent of Tuberculosis (TB) has infected a quarter of world's population and is among the leading cause of mortality from a single infectious pathogen after SARS CoV-2 [1]. Recent focus of TB research has shifted towards delineating the molecular functions of uncharacterized Mtb proteins that are determinants of immune response subversion and pathogen persistence [2, 3].

Mtb has adopted diverse strategies and evasion techniques for long-term survival within host's hostile intracellular niche. Co-evolving with the host, the pathogen possess effector proteins which are expressed at different stages of TB infection and are employed for dynamically modulating the host–pathogen interactions [4]. Several mycobacterial proteins are investigated for their role in disrupting host cell homeostasis via organelle targeting and for the presence of eukaryote-like domains to direct host pathways for pathogen survival. Mitochondria are crucial organelles involved in intrinsic programmed cell death pathways, therefore Mtb proteins targeting the mitochondria may have role in modulating apoptotic pathway and determining the outcome of infection [5].

About 7% of Mtb genome includes the recently evolved 107 PE (Pro-Glu) and 69 PPE (Pro-Pro-Glu) proteins which are preferentially present in pathogenic Mtb [6]. PE family proteins such as PE9-PE10 complex, PE_PGRS5, PE_PGRS11 and PE_PGRS26 proteins are reported to cause host cell apoptosis via targeting critical organelles like mitochondria and endoplasmic reticulum [7–10]. Autophagy, necrosis and apoptosis are the major cell death modalities studied so far with respect to PE family proteins; however, the induction of enhanced apoptosis by the PE family proteins have been implicated in spread of infection at the site of granuloma during late stages of infection [11]. Furthermore, a recent finding on PE_PGRS29 protein of Mtb has elucidated the presence of eukaryote-like ubiquitin-associated (UBA) domain within it which triggers xenophagy and controls bacterial load. These findings suggest that Mtb has evolved tactics where it takes control of intracellular bacterial load to limit host inflammatory responses for long-term intracellular survival [12].

PE family proteins have also been studied for establishment of the host–pathogen interaction due to their cell surface localization. These proteins are reported to bind to various Toll-Like-Receptors (TLRs) and aid in mounting a balanced immune response through activated macrophages which signals the migration of naïve immune cells at the site of granuloma and facilitate spread of infection [10]. Apart from their prominent role in maintenance of granuloma, the modulation of TLR-mediated immune response by these PE proteins have role in various cell processes such as cell death, antigen presentation and generation of oxidative stress [13–15].

Recently, PE6 (Rv0335c) protein has been reported to enhance TLR4 expression, evoke pro-inflammatory response, getting targeted to mitochondria and inducing caspase mediated intrinsic apoptosis in macrophages to facilitate pathogen survival [16]. Based on these recent findings on Rv0335c, we further investigated the role of Rv0335c in inducing mitochondrial perturbations and apoptosis by taking cues from the information encoded within protein's amino acid sequence. Through *in-silico* studies, we predicted that Rv0335c to have unique disordered C-terminal domain composed of hydrophobic amino acids similar to the C-terminal domain of mitochondrial targeted pro-apoptotic Bcl2 proteins in eukaryotes. The hydrophobic and disordered C-terminal domain in mitochondria targeting apoptotic Bcl2 proteins have been found to be responsible for their function [17, 18]. Additionally, the sequence scan of Rv0335c also showed the presence of two BH3-like motifs similar to those present in the eukaryotic Bcl2 proteins. One of these BH3-like motifs was found to be located at the C-terminal of protein. The Bcl2 proteins are master regulators of mitochondria-mediated intrinsic apoptosis and are characterized to possess conserved Bcl2 homology (BH)-domains. During apoptosis, pro-apoptotic multi-domain proteins such as Bax, Bak and BH3 only proteins such as Bid, Hrk and Bnip3 interact and activate each other via their BH3:BH3 groove [19, 20]. Since, the C-terminal domain of Rv0335c shared significant similarities with the apoptotic mitochondria-targeting Bcl2 proteins; we were prompted to investigate the role of C-terminal domain of Rv0335c in host cell death. Cloning, expression and purification of recombinant proteins (Rv0335c whole protein and Rv0335cΔCterm protein with deleted C-terminal domain) were performed followed by stimulation of THP1 macrophages for different time points. *In-silico* studies predicted Rv0335c to contain mitochondrial localization signal at its N-terminal. Confocal microscopy was performed which revealed that deletion of C-terminal domain from Rv0335c protein didn't affect its mitochondrial localization potential and both recombinant proteins (Rv0335c and Rv0335cΔCterm) were localized within mitochondria of THP1 macrophages. The impact of C-terminal domain of Rv0335c on mitochondria and its bioenergetics was assessed which showed that deletion of C-terminal from Rv0335c had insignificant effect on mitochondrial depolarization, levels of mitochondrial superoxides, cytosolic release of Cytochrome C (Cyt C) and intracellular ADP/ATP ratio in comparison to whole protein. Further, *in-silico* analysis predicted 9 calcium (Ca^{2+}) binding residues in Rv0335c and 4 of these residues were within the C-terminal domain which were deleted in Rv0335cΔCterm protein. THP1 macrophages stimulated with Rv0335cΔCterm protein showed insignificant intracellular Ca^{2+} influxes as compared to Rv0335c-stimulated cells. Additionally in comparison to Rv0335c, stimulation with Rv0335cΔCterm protein led to significant reduction in percentage of apoptotic cells as well as reduction in expression of Caspase 3, 7 and 9. Preliminary docking studies revealed that Rv0335c bound to immune receptor TLR4 with high affinity than Rv0335cΔCterm. We observed that the cell surface expression of TLR4 and HLA-DR along with soluble TNF-α were insignificant in response to Rv0335cΔCterm protein as compared to Rv0335c. All these findings unravel

the highly evolved strategy of molecular mimicry employed by Rv0335c protein of Mtb in causing host mitochondrial perturbations and apoptosis which may have implications on pathogen survival.

Materials and methods

In-silico evaluation of Rv0335c protein

Host cellular localization of Rv0335c protein

Rv0335c has recently been reported to get localized within host cell nucleus and mitochondria in a time dependent manner [16]. We also conducted *in-silico* analysis for probable cellular localization of Rv0335c protein within host cell using MemLoci server (Membrane Protein Subcellular Localization Predictor) (https://mu2py.biocomp.unibo.it/memloci/default/index) [21]. The server can predict whether the protein can be localized to plasma membrane, internal membrane (endoplasmic reticulum, nucleus, golgi apparatus, vesicles, vacuoles, lysosomes, peroxisome, microsomes, and endosome membranes) or organelle membrane (mitochondria). Mitofates server (http://mitf.cbrc.jp/MitoFates/cgi-bin/top.cgi) [22] was employed for identifying the presence of any putative mitochondrial pre-sequences and cleavage sites within Rv0335c.

Sequence scan and structure based comparative analysis of Rv0335c

Rv0335c was reported to target host mitochondria and induce apoptosis [16]. With this background information, a thorough sequence scan of Rv0335c protein was conducted. Prediction of disordered region within the protein was done using in PONDR server [23, 24].VL-XT algorithm was chosen in PONDR which trains the neural network based on non-redundant sets of ordered and disordered sequences incorporating attributes like hydropathy, composition and complexity of amino acids. For evaluating the hydropathy of protein, MINNOU server was used [25].

Defining the C-terminal domain in Rv0335c followed by homology modeling and structural superimposition

The C-terminal stretch from amino acid position 120 to 166 which was disordered, hydrophobic and posses one BH3-like motif was defined as C-terminal domain of Rv0335c protein. Based on similarities of C-terminal domain and BH3-like motif in Rv0335c with mitochondria-targeted pro-apoptotic Bcl2 proteins; multiple sequence alignment of C-terminal domain of mitochondria-targeted pro-apoptotic Bcl2 proteins and Rv0335c was done in ClustalW.

For homology modeling of Rv0335c protein as well as Rv0335cΔCterm protein, the sequences were submitted to I-TASSER server (https://zhanglab.ccmb.med.umich.edu/I-TASSER/) [26, 27]. Energy minimization of the generated models was done in Chiron (https://dokhlab.med.psu.edu/chiron/login.php) [28]. Structural validation of models was done based on scores of ERRAT, VERIFY3D and Ramachandran plot generated in PROCHECK [29–31].

Since, Rv0335c was found to contain a conserved BH3 motif similar to pro-apoptotic Bid and Hrk proteins; 3D structures of BH3 motif containing stretch from Bid and Hrk were superimposed with BH3-like motif containing C-terminal domain of Rv0335c using Pymol software.

Production of recombinant Rv0335c/Rv0335cΔCterm proteins and cell viability assays

Cloning, expression and purification of recombinant proteins

Rv0335c protein was PCR amplified from Mtb H37Rv genomic DNA using.

Forward Primer: Having BamHI site 5′ CTAGGATCC ATGTCGTTTGTCAACGTGG 3′.

Reverse Primer: Having HindIII site 5′ CTAAAG CTT GCCGTCGGCTCCGTTG 3′.

The Rv0355ΔCterm gene cloned in pMSQSCHS vector was a kind gift from Professor Vikas Jain [Department of Biological Sciences, Indian Institute of Science Education and Research (IISER) Bhopal]. Briefly, Rv0355ΔCterm gene was amplified with desired truncation from Mtb genomic DNA using the oligonucleotides:

(Forward Primer: 5′ ATGCGGTCCATGGGGTTCTTG CAC and.

Reverse Primer: 5′ ATGGTTCAGGTTCTGTGCAAA CTGGCCATGGAACG 3′).

PCR reaction was carried out and two sequential PCR reactions, one with Mtb genomic DNA and another with first PCR product were carried out in order to get desired Rv0335c genomic region. His-tag was added at the C-terminus of gene by cloning it with SmaI digested pMSQSCHS vector.

Rv0335c gene was cloned in pGEM T Easy vector (Promega) followed by its expression in pET-28a(+)vector (Novagen) with 6×His tag at N terminal. Both the genes (Rv0335c cloned in pET-28a(+)vector and Rv0355ΔCterm cloned in pMSQSCHS vector) were transformed in *E.coli* BL21 *DE3*. Recombinant proteins were purified from sonicated culture pellet after induction with 0.5 mM Isopropyl ß-D-1-thiogalactopyranoside using Ni–NTA affinity chromatography (Qiagen, USA) and elution was done with urea and different concentrations of immidazole. Eluted protein was dialyzed against 1XPBS and decreasing concentration

of urea to remove immidazole and urea. The purity was checked using SDS-PAGE and western blotting. Purified protein was further mixed and kept for binding with polymyxin agarose beads for endotoxin removal. Following incubation and centrifugation, the supernatant was collected and endotoxin contamination was checked using Limulus amoebocyte lysate kit (Thermo Fisher Scientific, USA) as per manufacturer's protocol. Protein concentration was estimated using BCA assay.

Culture of THP1 cell lines

Human monocytic cell line THP1 (NCCS, Pune) were plated in tissue culture plates in RPMI 1640 (Sigma) supplemented with 10% Fetal bovine serum (HiMedia), 1% HEPES (Sigma) and 50 µg/ml of Antibiotic (Life Technologies). The monocytic cells were treated with 40 ng/ml Phorbol-Myristate Acetate (PMA; Sigma) and incubated for 24 h to allow differentiation of macrophage.

(a) Cell Viability using CellTiter blue assays

For evaluating the dose dependent viability, THP1 macrophages were stimulated with different concentration (5 µg, 10 µg, 15 µg) of purified Rv0335c protein and incubated for 24 h. Cell viability was checked for 16 h, 24 h and 48 h following stimulation with 10 µg/ml of Rv0335c/Rv0335cΔCterm along with unstimulated cells and positive controls: LPS (40 ng/ml) and Staurosporine (2 µM). Following incubations, cells were subjected to either 20µL/well CellTiter Blue Reagent (Promega Corporation) and incubated for 4 h at 37 °C with 5% CO2 supply. Viable cells reduce CellTiter Blue reagent which is resazurin (dark blue) into resorufin (dark pink). The absorbance was measured spectrophotometrically at (570–600) nm. Percent of viability was calculated using absorbance values where unstimulated cells in media alone were considered to be 100% viable.

Localization studies of Rv0335c/Rv0335cΔCterm proteins within THP1 macrophages

THP1 macrophages (2×10^5) were grown on coverslips in a 24-well culture plate for microscopic studies. Following macrophage differentiation, cells were washed in 1xPBS and stimulated with Alexa Fluor™ 488-FITC (ThermoFisher Scientific) -labeled proteins. Unstimulated cells stained only with Alexa Fluor™ 488-FITC dye were included as negative control in the study. Briefly, approximately 500 µl of dialyzed proteins (2 mg/mL in 1xPBS) were incubated with 50µL of 1 M bicarbonate and reactive dye. After allowing the reaction to stir for 1 h at room temperature, dye bound proteins were purified through spin column centrifugation. After 6, 16 and 24 h post-stimulation with 10 µg/ml labeled proteins, cells were stained with MitoSpy Red CMXRos (BioLegend) and DAPI (BioLegend) as per manufacturer's protocol. Cells were washed in $1 \times PBS$, followed by fixation using 4% formaldehyde. Coverslip was washed again in $1 \times PBS$, mounted on glass slide and confocal microscopy was performed using Leica TCS SP8 microscope (Central Instrumentation Facility, South Campus, Delhi University). Cross-sectional images at step size of 0.5 micron of fluorescence signal was captured at 63X magnification for each sample. ImageJ was employed for analysis and quantification of confocal images. RGB plots, interactive surface plots and calculation of Pearson's coefficient through JACoP (Just Another Colocalization Plugin) plugin were done to analyse the mitochondrial localization of recombinant proteins. Statistical analysis was also performed between Pearson's coefficient values of Rv0335c and Rv0335cΔCterm proteins.

Mitochondrial perturbations in response to Rv0335c and Rv0335cΔCterm proteins

Changes in mitochondrial membrane potential (MMP) using JC-1 (5, 5′, 6, 6′-tetrachloro1, 1′, 3, 3′tetra-methyl-benzimidazolyl-carbocyanine iodide) dye

THP1 macrophages were left unstimulated/ stimulated with control/Rv0335c/Rv0335cΔCterm and incubated for 6 h, 16 h and 24 h. Following incubation, cells were resuspended in 1xPBS, stained with 2.5 µg of JC1 dye/ml and incubated at 37 °C for 30 min. Depending upon the membrane potential, JC1 dye accumulates in mitochondria. Monomeric form indicated by green fluorescence emission represents depolarized MMP and forms J-aggregates emitting red fluorescence MMP is hyperpolarized. Therefore, mitochondrial depolarization was indicated by decrease in red/green fluorescence intensity ratio of THP1 macrophages using BD Accuri C6 flow cytometer by collecting 10,000 events for each sample.

Estimation of mitochondrial superoxide generation using MitoSox Red dye

THP1 macrophages were left unstimulated/ stimulated with control/Rv0335c/Rv0335cΔCterm and incubated for 6 h, 16 h and 24 h. Following incubation, cells were re-suspended in 1xPBS, stained with 3.5uM of MitoSOX red dye and incubated at 37 °C for 30 min. MitoSOX™ Red (ThermoFisher Scientific) is a live cell permeable dye which selectively targets mitochondria where it gets oxidized by mitochondrial superoxide and emits fluorescence.

Mitochondrial superoxide production was estimated in terms of percentages of cells positively stained for MitoSOX dye using BD accuri C6 flow cytometer by collecting 10,000 events for each sample.

Estimation of cytosolic release of Cyt C

In healthy cells, Cyt C resides within the mitochondrial membrane. Mitochondrial stress and apoptotic stimuli induce the cytosolic release of Cyt C from mitochondrial membrane. Unstimulated/control/protein stimulated THP1 macrophages were incubated for 16 h, 24 h and 48 h. Harvested cells were washed and fixed in 4% para-formaldehyde for 15 min at room temperature following which cells were permeabilized in perm buffer for 15 min at room temperature. FITC labeled Anti-Cytochrome C antibody (Clone-6H2, Thermo Fisher Scientific) was used to stain the cells in residual buffer volume and incubated at 4 °C for 1 h and acquired in BD accuri C6 flow cytometer.

Changes in intracellular ratio of ADP/ATP

Mitochondrial stress also affects the bioenergetics of mitochondria and alters ADP/ATP ratio. Changes in ADP/ATP ratio is also used for detecting the modality of cell death and viability. Apoptotic cells are screened by elevated levels of ADP and depleted levels of ATP. Detection of ADP/ATP ratio in unstimulated/control/protein stimulated THP1 macrophages was performed at 24 h and 48 h according to manufacturer's protocol (Sigma-Aldrich). Briefly, the cells were lysed to release ATP and ADP. ATP directly reacts with the substrate D-luciferin and produces light in presence of luciferase which is an indicator of intracellular ATP levels. In the next step, the ADP is converted to ATP which then undergoes the same reaction and produces second light intensity that represents the total ADP and ATP concentration in the sample. Ratio of luminescence light intensity of unstimulated/stimulated was taken as a measure of intracellular ADP/ATP measurement with unstimulated ADP/ATP ratio taken as 1.

Ca^{2+} binding affinity and impact of intracellular calcium homeostasis in response to protein stimulation

Ca^{2+}is a crucial signaling molecule that maintains the intracellular homeostasis by regulating Ca^{2+}release and uptake by organelles like endoplasmic reticulum and mitochondria.

Prediction of calcium binding affinity of Rv0335c protein

Rv0335c protein's sequence was evaluated for its affinity to bind calcium ligand in MIB server (http://bioinfo.cmu.edu. tw/MIB/) [32].

Intracellular Ca^{2+} influx in response to Rv0335c/ Rv0335cΔCterm proteins

Unstimulated/control/Rv0335c/Rv0335cΔCterm protein stimulated THP1 macrophages were cultured and incubated for 16 h and 24 h. Cells were harvested and Indo-1, AM (ThermoFisher Scientific) dye (2 μM)was added to cell suspension and incubated at 37 °C for 15–60 min.Indo-1, AM is a cell permeable sensitive indicator dye of intracellular Ca^{2+}levels, which allows the cleaving of AM esters by cellular esterases after crossing the plasma membrane. This makes the dye cell impermeant and thus stuck inside the cells. The Ca^{2+} influx was measured by estimating the ratio of fluorescence intensity using a 494-nm excitation (bound Ca$^{2+)}$. As a positive control, Ionomycin (10 μg/ml) was added prior to acquisition in one of the cultured THP1 cell suspension.

Apoptotic cell death induction by Rv0335c and Rv0335cΔCterm proteins

Evaluation of phosphatidyl-serine exposure using annexin V-FITC staining and TUNEL Assay for DNA fragmentation in THP1 macrophages

Early apoptosis is marked by the flipping of Phosphatidylserine on the outer cell membrane. Following stimulation (16 h, 24 h and 48 h), unstimulated/stimulated THP1 macrophages were stained with Annexin V-FITC/Propidium iodide (PI) using Annexin V-FITC apoptosis detection kit (Thermo Scientific) following manufacturer's protocol analyzed using flow cytometer (BD AccuriC6). For each sample, total 10,000 events were collected and appropriate gating was used to measure the fluorescence of FITC and PI. Cells with three phenotypes, i.e., normal viable (AnnexinV-/PI-cells), early apoptotic (AnnexinV+/PI-cells), and late apoptotic (AnnexinV+/PI+cells) within a mixed cell population were observed.

Unstimulated/stimulated THP1 macrophages were incubated for 24 h. For detecting DNA breaks in apoptotic cells; APO-Direct kit (BD Pharmingen) was used according to the manufacturer's protocol. Briefly, cells were fixed using 1% para-formaldehyde and incubated for 60 min on ice. After washing with ice cold 1xPBS, fixed cells were re-suspended in 70% ethanol and incubated for 30 min on ice and stored

at − 20 °C for 18–24 h. Cells were then washed and labeled with 50 µl DNA labeling solution containing Terminal deoxynucleotidyl transferase (TdT) enzyme and FITC-dUTP in reaction buffer. TdT is a polymerase that catalyses the addition of FITC-dUTP at the 3'-OH end of the fragmented DNA. Cells were rinsed and dissolved in PI/RNase Staining Buffer following incubation for 30 min at room temperature in dark. Percentage of cells with fragmented DNA or percentage of TUNEL positive cells were recorded from total 10,000 events collected for each sample.

Detection of activated initiator caspase 9 and executioner caspase 3 and caspase 7

Following 24 h of protein stimulation, total protein was extracted by lysing of THP1 macrophages using RIPA lysis buffer mixed with protease inhibitor cocktail (Santa Cruz Biotechnology Ltd.). Total protein concentration of whole cell lysate was determined and equal concentration of samples were loaded and subjected to SDS-PAGE followed by transferring onto nitrocellulose membrane. Membranes were blocked for 1 h in 5% skimmed milk dissolved in Tris-buffered saline with Tween 20 (TBST) buffer followed by overnight incubation in primary polyclonal antibody to Caspase 9 (PAA627Hu03, Cloud-Clone Corp.), and GAPDH (Thermo Scientific) as an internal control, dilution 1:1000. Membranes were washed in TBST buffer prior to incubation with HRP conjugated secondary antibody for 1 h. The blot was developed using a super-sensitive ECL Chemiluminescence Kit (Thermo Scientific). Western Blotting images were also quantified using ImageJ software. The developed band area for each sample was analyzed and graphs were plotted in terms of ratio with respect to unstimulated sample.

Unstimulated and protein stimulated THP1-macrophages were incubated for different time points (16, 24 and 48 h). CellEvent Caspase-3/7 Green Flow Cytometry Assay kit (Invitrogen) was used to detect activation of executioner caspase 3 and caspase 7 according to manufacturer's protocol. Cell event caspase 3/7 reagent (500 nM) was added to 1 ml cell suspension in 1xPBS and incubated for 30 min at 37 °C. SYTOX dead cell stain (1 µM) was added 5 min before acquisition of samples in BD accuri C6 flow cytometer.

For inhibition studies, cells were pre-incubated with 20 µM total caspase inhibitor (Z-VAD-fmk; Promega) for 1 h followed by stimulation with proteins/controls and incubated for 24 h. Percentage of caspase 3 and 7 activation was recorded from total 10,000 events acquired for each sample. To ascertain that the observed apoptosis is caspase-mediated, we also studied the percentage of apoptosis in caspase inhibitor treated THP1 macrophages.

Immune response generated in response to recombinant Rv0335c/Rv0335cΔCterm proteins

TLR identification in Rv0335c interaction predicted from molecular docking

Rv0335c/Rv0335cΔCterm docking studies with human TLR4 (PDB ID 3FXI) protein structures were performed in Haddock server. Best structures were visualized in Discovery Studio Visualizer 4.1.

TLR4 and HLA-DR expression profiles in response to Rv0335c/Rv0335cΔCterm proteins

THP1 macrophages were left unstimulated or stimulated with control/Rv0335c/Rv0335cΔCterm proteins for evaluating the surface expression of TLR4 following 24 h of incubation. LPS-a TLR4 agonist (40 ng/ml) was included as positive control and Mtb Cell Wall fraction (CWF) was included as negative control. For staining the antibodies used were-APC labelled anti-human TLR2 (CD282) antibody (Thermo Scientific) or APC labeled anti-human TLR4 (CD284) antibody (Thermo Scientific) and PE labeled anti-human HLA-DR antibody (eBiosciences, Germany). Acquisition of cells was done in BD accuri C6 flow Cytometer (BD, USA) and percentage positive stained cells were analyzed.

For inhibition studies, cells were pre-treated with Anti-TLR4 monoclonal antibody (Thermo Scientific) 1 h prior to stimulation with proteins and expression of TLR4 and HLA-DR were estimated after 24 h using flow cytometry.

Evaluation of pro-inflammatory cytokines TNF-α and IL-1β

ELISA was performed according to manufacturer's protocol with cell culture supernatants of THP1 macrophages which were left unstimulated or stimulated with control or Rv0335c/Rv0335cΔCterm proteins for 16 h, 24 h and 48 h for secretion of TNF-α (Thermo Scientific) and IL-1β (BioLegend).

Statistical analysis

Results are presented as Mean ± SEM of three independent experiments. Student's t-test was employed for comparisons using Graph Pad Prism software version 5.02 (San Diego, CA, USA). The differences in mean were analyzed where* represents comparison with unstimulated

while # represents comparison between Rv0335c and Rv0335cΔCterm. [(#,*) P < 0.05, (##,**) P < 0.01, (###,***) P < 0.001, (####,****) P < 0.0001].

Results

In-silico studies predicted presence of mitochondrial localization sequence at N terminal of Rv0335c; and presence of hydrophobic, disordered C-terminal domain with BH3-like motif similar to mitochondrial targeted pro-apoptotic Bcl2 proteins

Rv0335c protein targets host mitochondria

As reported by *Sharma* et al.*,* our *in-silico* analysis also confirmed the mitochondrial targeting potential of Rv0335c protein. MemLoci server predicted the localization of Rv0335c protein in the organelle's membrane i.e., mitochondrial membrane. Predictions of MitoFates server revealed that Rv0335c protein has mitochondrial targeting pre-sequence and cleavage site for mitochondrial processing peptidases which is predicted to cleave the pre-sequence at Proline residue (33 amino acid position) of Rv0335c protein. Mitochondrial processing peptidases is an enzyme complex of mitochondria that cleaves signal sequences in mitochondria targeting proteins. Rv0335c protein is also predicted to have TOM20 recognition motif (LHRAC sequence positioned from 7 to 11 amino acid residues) (Fig. 1). TOM20 is receptor for mitochondrial targeted protein which recognizes and cleaves the targeting protein pre-sequence.

Rv0335c protein has C-terminal domain and BH3-like motif similar to mitochondria-targeted pro-apoptotic Bcl2 proteins of eukaryotes

Sequence scan of Rv0335c predicted that the protein was mostly unstructured/disordered and hydrophobic. Rv0335c also was predicted to have two BH3-like motifs which were characterized by presence of typical L-X-X-X-X-D amino acid sequence (from amino acid sequence 73 to 78 and from 134 to 139)[17, 20, 33]. One of these BH3-like motifs is present at the C-terminal of Rv0335c protein (Fig. 2a). Literature analysis pointed out that almost all the mitochondrial targeted pro-apoptotic Bcl2 proteins (Bak, Bax, Bad, Bim, Bid, Hrk (Dp5), PUMA, NOXA, Beclin1, Bnip3) are intrinsically unstructured/disordered which helps in protein–protein interaction and are characterized by the presence of hydrophobic C-terminal domain which plays significant role in mitochondrial targeting and apoptosis [25]. Based on these observations and significant similarities between the C-terminal domain of Rv0335c and mitochondrial targeted pro-apoptotic Bcl2 family proteins, it was hypothesized that the hydrophobic, disordered C-terminal domain containing single BH3-like motif in Rv0335c may be involved in mitochondria-mediated intrinsic apoptosis inducing function of this protein (Fig. 2b).

Defining the C-terminal domain in Rv0335c along-with homology modeling and structural similarities

The C-terminal of Rv0335c protein was mostly disordered, hydrophobic and contains a terminally located BH3-like motif and therefore, a stretch of amino acid position 120 to 166 was defined as the C-terminal domain of R0335c protein (Fig. 3a). Multiple sequence alignment showed sequence

Presequence
- Possessing mitochondrial presequence (Precision:0.83, Recall:0.73)
- Possessing mitochondrial presequence (Precision:0.79, Recall:0.80)
- No mitochondrial presequence

Cleavage site
- MPP cleavage site
- Oct1 cleavage site
- Icp55 cleavage site

Motif
- TOM20 recognition motif (ΦχβΦΦ)
- Max positively charged amphiphilicity (PA) score region (high)
- Max positively charged amphiphilicity (PA) score region (low)
- Φ β σ Y Reduced letters composing statistically significant 6mer in presequence Φ(hydrophobic), β(basic), σ(polar), γ(secondary structure breaker)

Sequence ID	Probability of presequence	Cleavage site (processing enzyme)	Net charge	Sequence (100 amino acids from N terminal)
Rv0335c|PE6	0.889	33 MPP	0.182	VRSMGFLHRACRAPSSLPAPLMARPGRSVLARPAATPPGPLCATTRPRPPQGNQPPASRISNFPPKRHKT

Fig. 1 Mitochondrial localization of Rv0335c protein predicted by MitoFates server. Rv0335c protein is predicted to contain mitochondrial targeting pre-sequence with cleavage site for mitochondrial processing peptidases and recognition site for TOM20 in MitoFates server (Color figure online)
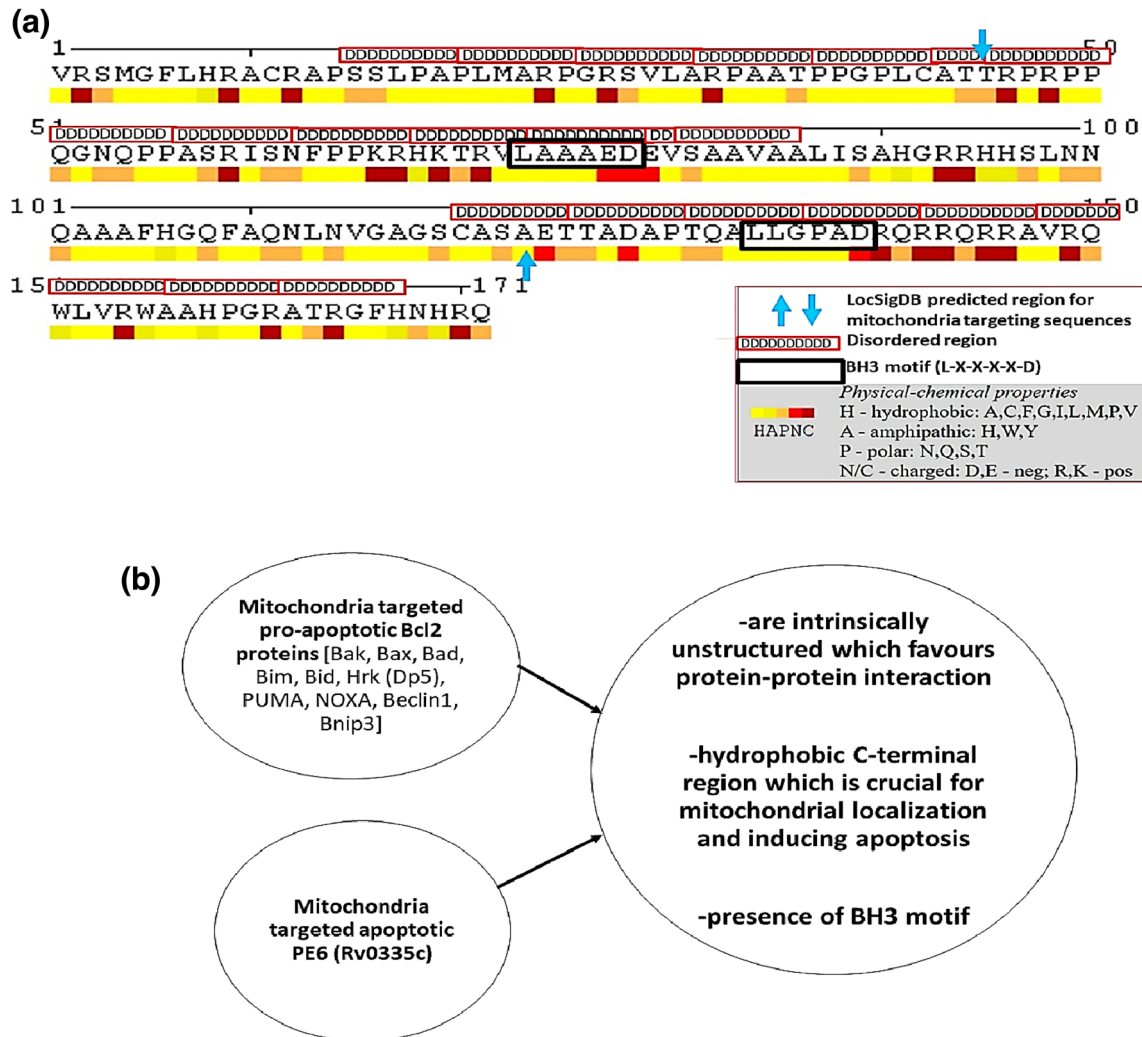
Fig. 2 Rv0335c protein is mostly disordered, hydrophobic, contains BH3-like motif and has similarities with mitochondria targeting pro-apoptotic eukaryotic Bcl2 proteins. **a** Rv0335c protein was predicted to be mostly disordered and composed of hydrophobic amino acid residues. Additionally, the protein was found to contain two typical BH3-like motifs. BH3 motifs are exclusive in eukaryotic Bcl2 proteins. **b** Rv0335c protein of Mtb shares similarities with mitochondria targeted pro-apoptotic Bcl2 proteins in terms of being intrinsically unstructured, hydrophobic C-terminal domain and presence of BH3 motifs (Color figure online)

similarities between the C-terminal domain of Rv0335c and C-terminal domain of different mitochondria targeting Bcl2 family proteins involved in apoptosis (Fig. 3b).

Secondary structure prediction and homology modelling for Rv0335c and Rv0335cΔCterm proteins were done using I-TASSER server which generated 5 models. All these models were subjected to Chiron server for energy minimization. Model with a good C score in I-TASSER, > 95% residues in favored region as predicted in Ramachandran plot, good Errat and Verify3D scores was selected for both proteins.

Multiple sequence alignment revealed that the BH3-like motif at C-terminal domain of Rv0335c was completely aligned and conserved with the BH3 motif of pro-apoptotic mitochondria targeted Bid and Hrk proteins. Structural superimposition showed that the BH3-like motif containing C-terminal domain of Rv0335c was structurally aligned with the BH3-motif containing stretch of Bid and Hrk proteins (Fig. 3c).

Cloning, expression and purification of recombinant proteins

Cloning of His-tagged recombinant Rv0335c in pET28a(+) expression vector and Rv0335cΔCterm in pMSQSCHS expression vector transformed in BL21 *DE3* was successful and validated by sequencing. By affinity chromatography, both recombinant proteins were purified from the insoluble fraction of BL21 *DE3* culture. Rv0335c had a molecular weight of 18.3 kDa and Rv0335cΔCterm protein had a molecular weight of approximately 12.8 kDa as determined

by SDS-PAGE and western blotting using anti-His antibody (Fig. S1). One liter of culture yielded approximately 1.5 mg/mL of protein. Removal of bacterial endotoxin from purified protein was performed by passing the protein fractions through polymyxin B-agarose beads. Limulus Amoebocyte Lysate assay (Pierce, USA) was performed for the collected fractions, which revealed almost negligible endotoxin contamination (0.20 EU/ml for Rv0335c protein and 0.16 EU/ml for Rv0335cΔCterm protein).

C-terminal domain in Rv0335c protein has role in inducing cell death of THP1 macrophages

Cell viability was estimated with CellTiter Blue assay to check the viability of THP1cells in response to our protein stimulations. Initially, three different concentrations of Rv0335c protein (5 μg/ml, 10 μg/ml and 15 μg/ml) were used in stimulation for dose dependent viability estimation. Rv0335c was found to significantly affect the viability of THP1 macrophages in a dose dependent manner [Figure S2 (a)]. We selected 10 μg/ml of protein stimulation for our further experiments. Two controls namely Lipo Poly-Saccharide (LPS) and Staurosporine were included as positive controls in all our experiments unless mentioned otherwise. In case of time dependent viability, both Rv0335c and Rv0335cΔCterm-stimulated cells showed significant loss of cell viability in comparison to unstimulated cells but the loss of viability in Rv0335cΔCterm-stimulated cells was less as compared to Rv0335c protein. At 24 h and 48 h, we observed a significant ~ 14 to 20% decrease in cell viability in response to Rv0335c as compared to Rv0335cΔCterm protein [Fig. S2 (b)]. Our observations suggest a possible role of C-terminal domain of Rv0335c protein which majorly affects cell viability and cause cell death of THP1 macrophages.

C-terminal domain in Rv0335c partially contributes to protein's localization to mitochondria

For localization studies, we used Alexa-fluor 488 labeled recombinant proteins to stimulate THP1 macrophages up to 24 h and performed confocal microscopy. Unstimulated cells with only Alexa-fluor 488 stain were used as controls in the microscopic study. We observed that both Rv0335c and Rv0335cΔCterm proteins were localized within the mitochondria starting 6 h of protein stimulation in a time dependent manner. Pearson's coefficient values suggest a linear relationship in the intensity of Mitospy CMXRos and Alexafluor488 labelled protein indicating the colocalization of Rv0335c with mitochondria of THP1 macrophages. Pearson's coefficient values for Rv0335cΔCterm protein also suggest its localization to mitochondria though the Pearson's coefficient values were not as high as observed for Rv0335c

protein (Fig. 4a–c). The difference in Pearson's coefficient values of Rv0335c and Rv0335cΔCterm protein were significantly different. These findings suggest that the deletion of C-terminal domain in Rv0335c protein accounts for to its localization to host mitochondria but partially because of intact N terminal mitochondrial targeting sequence in Rv0335cΔCterm protein.

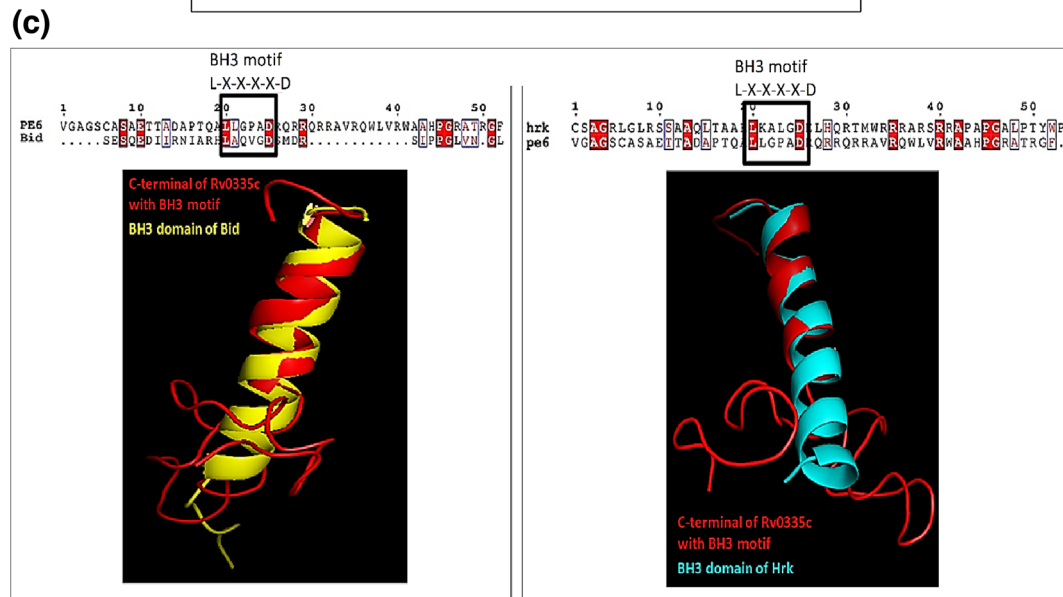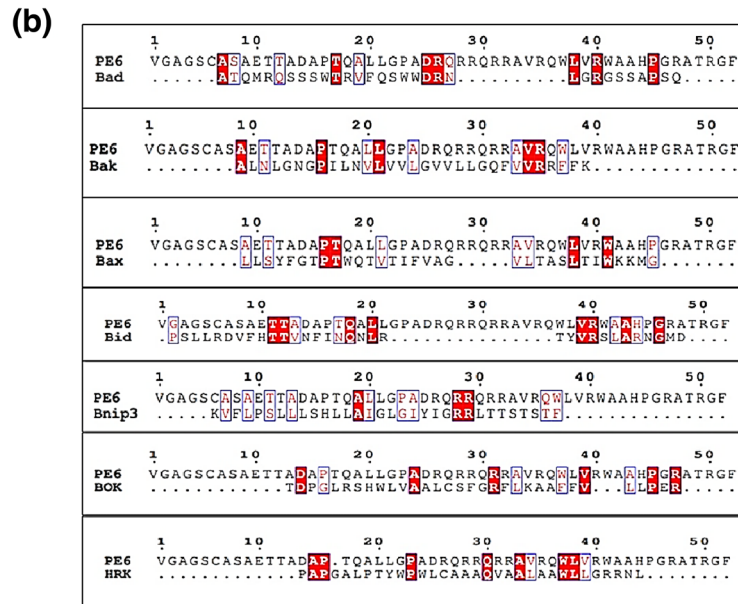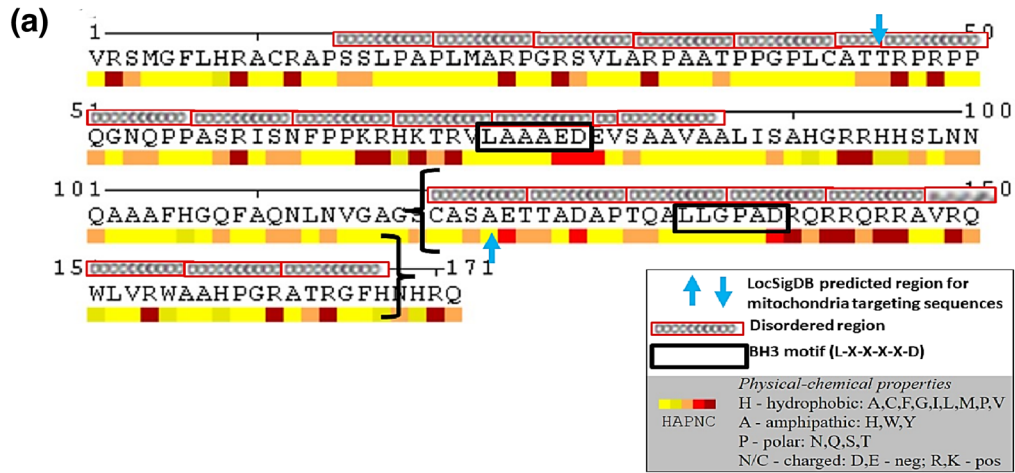## C-terminal domain in Rv0335c induced high levels of depolarization of MMP

Alterations in mitochondrial membrane integrity can be studied by estimation of MMP and is indicative of mitochondrial related perturbations. Rv0335c protein led to significant depolarization of MMP starting at 6 h till 24 h of study. In case of Rv0335cΔCterm protein, we found that this depolarization of MMP was not very pronounced as compared to Rv0335c whole protein. MMP was studied in terms of red/green fluorescence ratio, and we observed a significant decrease (~ 1.5-to-twofold) in levels of MMP depolarization in response to Rv0335cΔCterm protein than Rv0335c whole protein till 24 h of study (Fig. 5a and 5b).

C-terminal domain in Rv0335c caused increased levels of mitochondrial superoxides

Mitochondrial stress leads to the leakage of electrons from electron transport chain within the mitochondrial membrane. These leaked electrons combine with oxygen to generate mitochondrial superoxides. Depolarization of MMP, followed by superoxide are some of the early and transient steps that ensure that cells will irrevocably undergo intrinsic apoptosis. There was a significant increase in the level of superoxides in Rv0335c stimulated THP1 macrophages as compared to unstimulated cells at all the time points. We observed a comparable level of superoxide production in response to Rv0335cΔCterm protein when compared to unstimulated cells at 6 h. At 16 h and 24 h, the superoxide production in response to Rv0335cΔCterm protein increased slightly in comparison to unstimulated cells. However, in comparison to Rv0335c protein, superoxide levels in response to Rv0335cΔCterm protein were significantly lower (~ 1.5-fold) till 24 h of study (Fig. 5c, d).

C-terminal domain in Rv0335c caused increased intracellular ratio of ADP/ATP in THP1 macrophages

Mitochondrial ATP generation is reduced in apoptotic cells with inhibited mitochondrial activities, resulting in heightened cytosolic ADP/ATP ratios. Using a plate-based bioluminescence assay, changes in the ADP/ATP ratio in THP1 cells stimulated by Rv0335cΔCterm/Rv0335c proteins were calculated. We observed increased ADP/ATP ratio in

(a)

```
1                                                    50
VRSMGFLHRACRAPSSLPAPLMARPGRSVLARPAATTPPGPLCATTRPRPP
HAPNC

51                                                  100
QGNQPPASRISNFPPKRHKTRV LAAAED EVSAAVAALISAHGRRHHSLNN

101                                                 150
QAAAFHGQFAQNLNVGAG CASAETTADAPTQA LLGPAD QRRQRRAVRQ

151        171
WLVRWAAHPGRATRGFHNHRQ
```

Legend:
↑↓ LocSigDB predicted region for mitochondria targeting sequences
Disordered region
BH3 motif (L-X-X-X-D)

Physical-chemical properties
HAPNC
H - hydrophobic: A,C,F,G,I,L,M,P,V
A - amphipathic: H,W,Y
P - polar: N,Q,S,T
N/C - charged: D,E - neg; R,K - pos

(b)

(c)

C-terminal of Rv0335c with BH3 motif
BH3 domain of Bid

C-terminal of Rv0335c with BH3 motif
BH3 domain of Hrk

◄**Fig. 3** Defining the C-terminal domain in Rv0335c followed by its multiple sequence alignment and structural superimposition with eukaryotic pro-apoptotic Bcl2 proteins. **a** The C-terminal domain in Rv0335c protein was defined from amino acid position 120 to 166 in brackets ({}). This stretch was disordered, hydrophobic and contains a terminally located BH3-like motif in Rv0335c protein. **b** Multiple sequence alignment of C-terminal domain of Rv0335c and C-terminal domain of mitochondria targeted eukaryotic pro-apoptotic Bcl2 proteins. **c** Multiple sequence alignment and structural superimposition of BH3-like motif containing C-terminal domain of Rv0335c with BH3 motif containing stretch of mitochondria targeted eukaryotic pro-apoptotic Bid and Hrk proteins (Color figure online)

response to Rv0335c as compared to unstimulated cells and this increase was significant at 24 h and 48 h. In response to Rv0335cΔCterm protein, the ADP/ATP ratio was comparable to the unstimulated cells till 48 h of study. It was observed that Rv0335cΔCterm led to significant decrease (~ 1.6 to twofold) in ADP/ATP ratio when compared to Rv0335c protein at all the time points (Fig. 6a).

C-terminal domain in Rv0335c caused increased levels of cytoplasmic Cyt C

Mitochondrial perturbations have been shown to result in the release of Cyt C from the mitochondrial membrane into the cytoplasm, indicating that mitochondrial membrane integrity has been compromised. We observed a time dependent increased levels of cytoplasmic Cyt C in Rv0335c stimulated THP1 macrophages at all the time points in comparison to unstimulated cells. The cytosolic Cyt C levels in response to Rv0335cΔCterm were comparable to the unstimulated cells at all the time points. We observed a significant decrease in cytosolic release of Cyt C (~ 15 to 25%) till 48 h of Rv0335cΔCterm stimulation in comparison to Rv0335c protein stimulation (Fig. 5 e, f).

MitoSpy CMXRos dye is used for mitochondrial localization studies and its function is based on mitochondrial membrane potential. When we observed the RGB plots of our confocal microscopy images, we found a gradual decrease in the intensity of MitoSpy CMXRos staining in a time dependent manner which was very prominent in case of Rv0335c stimulation. At 6 h the intensity of MitoSpy CMXRos observed in Rv0035c stimulated cells was 140 which significantly reduced to ~ 70 after 24 h of Rv0335c stimulation. In case of Rv0335cΔCterm protein stimulation, this decrease in intensity of MitoSpy CMXRos was less prominent (~ 120 at 6 h, 140 at 16 h and 100 at 24 h) (Fig. 4b). Therefore, our confocal microscopy analysis results corroborated with our finding of loss of mitochondrial membrane integrity (depolarized MMP, generation of mitochondrial superoxides and cytoplasmic Cyt C release) which indicate significant mitochondrial perturbations and declining macrophage cell health in response to Rv0335c protein of Mtb.

C-terminal domain in Rv0335c was predicted to have Ca²⁺ binding residues and played role in modulating the intracellular Ca²⁺ influx in THP1 macrophages

C-terminal domain in Rv0335c was predicted to have 4 Ca²⁺ binding residues

Rv0335c was analyzed for its calcium binding affinity using MIB server. We observed 9 residues with high calcium binding affinity within whole Rv0335c protein. Four residues- 125 Thr, 128 Asp, 140 Arg, 141 Gln, which were within the C-terminal domain of protein were deleted in Rv0335cΔCterm protein (Fig. 6b).

C-terminal domain in Rv0335c increased the intracellular Ca²⁺ influx in THP1 macrophages

Studies have reported the presence of Ca^{2+} binding motifs within PE_PGRS subfamily of PE/PPE proteins [34, 35]. Ca^{2+} binding in Mtb proteins disrupt Ca^{2+} homeostasis modulating ER-mitochondrial Ca^{2+} fluxes leading to apoptotic cell death. Since, Rv0335cprotein was predicted to contain 9 Ca^{2+} binding motifs, we evaluated the intracellular Ca^{2+}levels in response to Rv0335c/Rv0335cΔCtermproteins using flow cytometry-based staining with Indo-1AM dye. We observed a significant increase in intracellular Ca^{2+} levels in Rv0335c stimulated THP1 macrophages in comparison to unstimulated cells at all the time points of study. However, in case of Rv0335cΔCterm protein with only 5 Ca^{2+} binding residues, this increase in Ca^{2+} levels were not significant as compared to unstimulated cells. Intracellular Ca^{2+} levels were significantly decreased (~ 1.48-fold) at 16 h and (~ 1.25-fold) at 24 h in response to Rv0335cΔCterm protein as compared to Rv0335c protein (Fig. 6c, d).

C-terminal domain in Rv0335c led to enhanced caspase-mediated apoptotic cell death

C-terminal domain in Rv0335c induced increased apoptosis of THP1 macrophages

The flipping of phosphatidylserine (PS) from the inner to the outer leaflet of the plasma membrane is one of the biochemical alterations associated with the triggering of apoptosis. Rv0335cprotein resulted in a gradual time-dependent increase in cells undergoing early apoptosis (annexinV positive cells in Fig. 7b, bottom right quadrant) and late apoptosis (annexinV/PI dual-positive cell population in Fig. 7b, top right quadrant) in comparison to the unstimulated cells. In response to Rv0335cΔCterm protein the percentage of annexinV positive cells were comparable to the unstimulated cells at 16 and 24 h. We
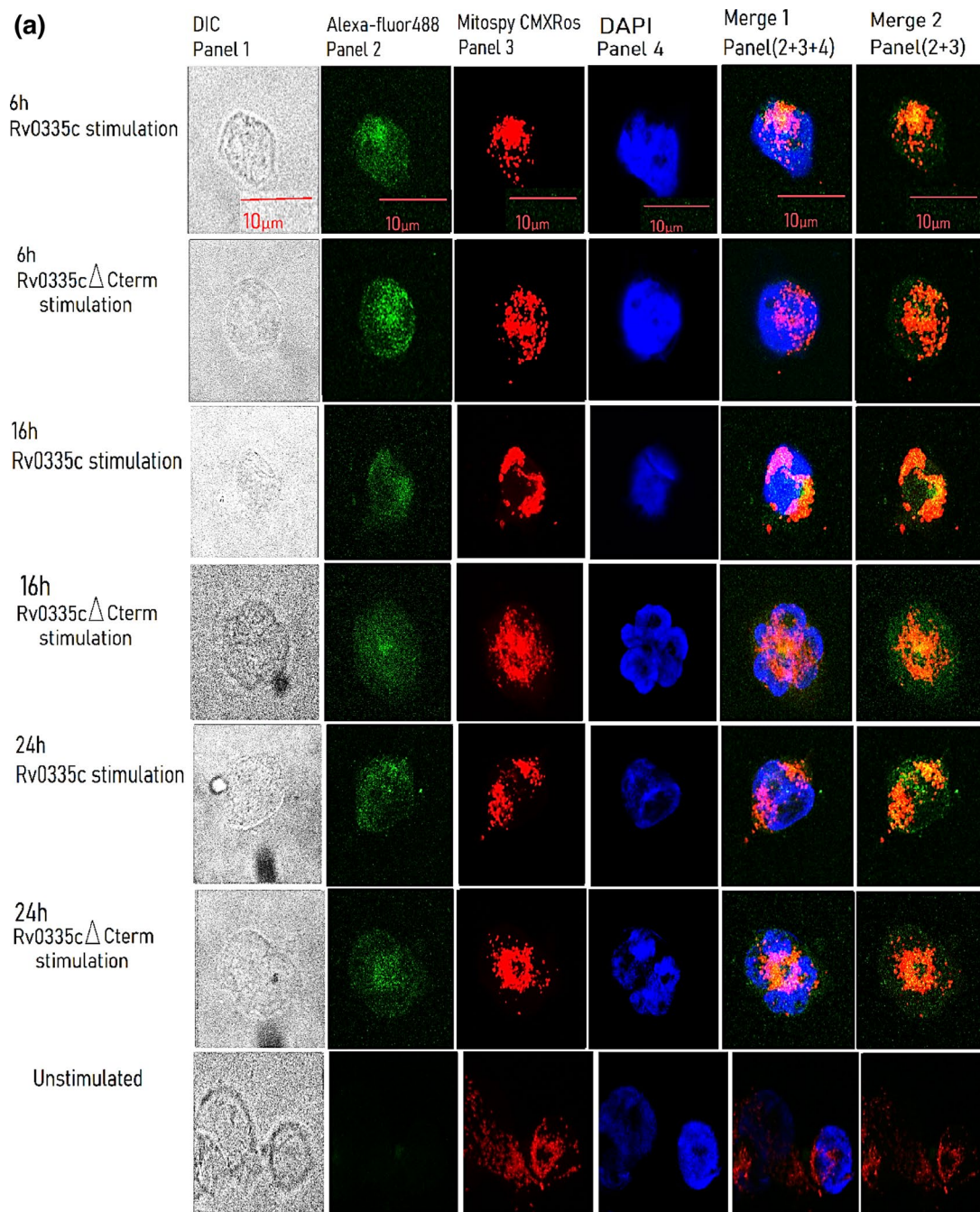
Fig. 4 Confocal microscopy analysis showing the mitochondrial localization of recombinant proteins. THP1 macrophages were left unstimulated stained with Alexa-fluor488 dye/Alexa-fluor488-labeled Rv0335c protein/Alexa-fluor488-labeled Rv0335cΔCterm protein and incubated till 24 h. Following stimulation, cells were stained with MitoSpy Red CMXRos followed by DAPI as per manufacturer's protocol and fixed in 4% formaldehyde. Confocal microscopy confirmed the localization of both Rv0335c and Rv0335cΔCterm proteins within mitochondria of THP1 macrophages. **a** Confocal microscopy (cross-sectional images of fluorescence signal at step size of 0.5 micron and 63X magnification) confirmed the localization of recombinant proteins within mitochondria of THP1 macrophages [Panel 1: Differential interface contrast image, Panel 2: Alexafluor488 labeled protein stimulation/ only Alexafluor488 dye in unstimulated, Panel 3: Mitospy CMXRos mitochondrial dye, Panel 4: DAPI nuclear stain, Merge 1: Panel (2+3+4), Merge 2: Panel (2+3)]. **b** Cross-sectional confocal images were analyzed in ImageJ software and RGB plots and 3D surface plot depicting the fluorescence intensity showed higher mitochondrial localization of recombinant proteins in a time dependent manner (**c**) JACoP (Just Another Colocalization Plugin) plugin in ImageJ was used to calculate the Pearson's Coefficient (r) of mitochondrial localization of recombinant proteins. RGB Plot depicts a time dependent decrease in MitoSpy CMXRos dye intensity indicating a time dependent decrease in mitochondrial membrane potential (Color figure online)
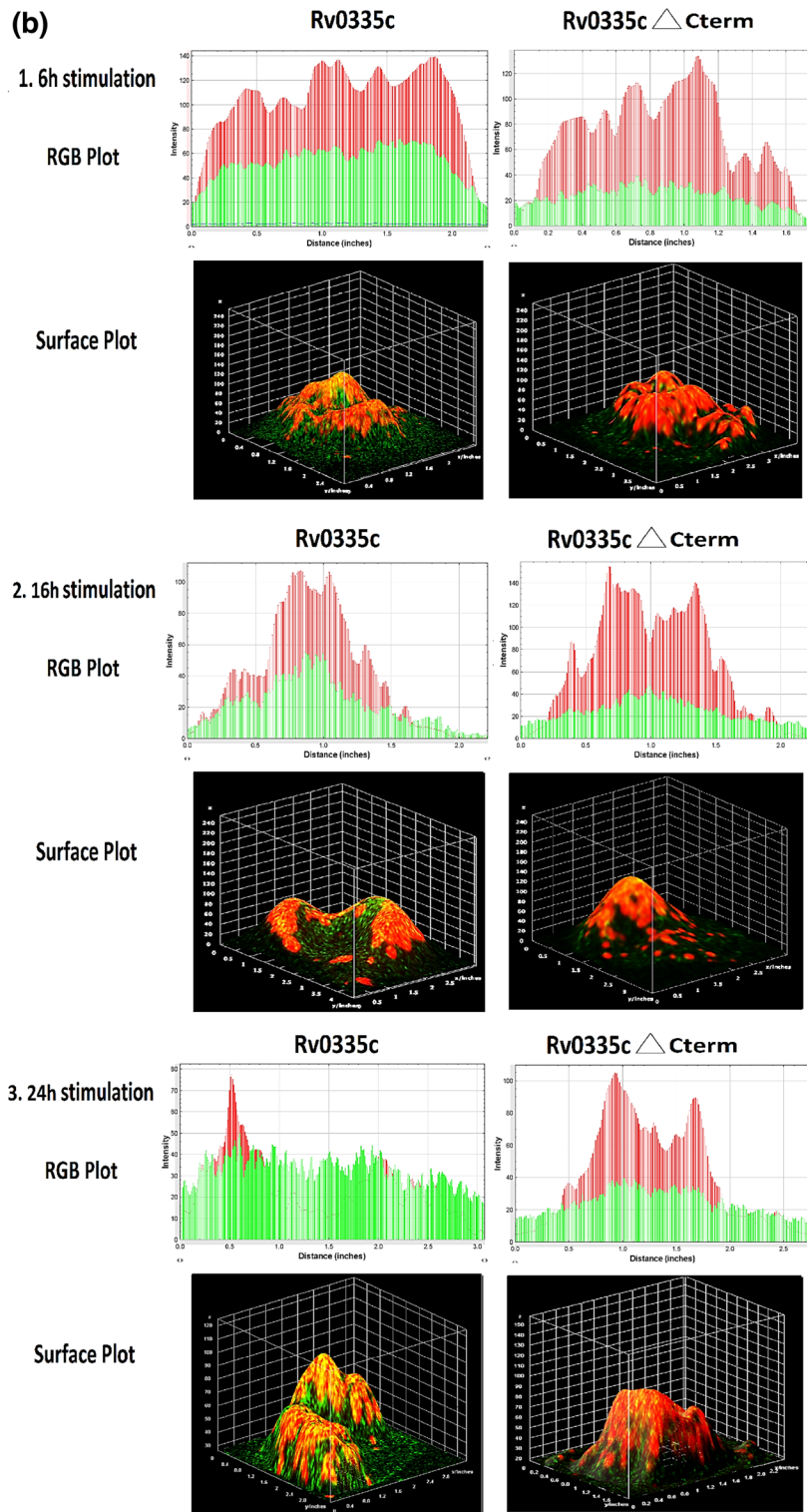
Fig. 4 (continued)

observed significant decrease in the percentage of apoptosis (~ 15 to 20%) in response to C-terminal domain deleted Rv0335cΔCterm protein than Rv0335c at 24 h and 48 h (Fig. 7a). We observed a slight increase in percentage of cells undergoing apoptosis in response to Rv0335cΔCterm when compared to unstimulated cells at 48 h. However, the percentage of cells undergoing apoptosis in Rv0335cΔCterm stimulated THP1 macrophages

(c)

Time point	Pearson's Coefficient value (r)		P value	Statistically significant
	Rv0335c	Rv0335cΔCterm		
6H	0.724	0.469	0.0039	Yes
16H	0.786	0.542	0.0033	Yes
24H	0.957	0.599	0.0009	Yes

Fig. 4 (continued)

were significantly low at all the time points in comparison to Rv0335c protein.

DNA fragmentation is a distinct marker of cells undergoing apoptotic cell death and was also studied by TUNEL assay after 24 h of stimulation. We observed a significant percentage of TUNEL positive cells in Rv0335c protein in comparison to unstimulated cells. Rv03355ΔCterm protein stimulation showed comparable levels of TUNEL positive cells as unstimulated cells. There was significant decrease (~1.3-fold) in TUNEL positive cells in response to Rv03355ΔCterm protein than Rv0335c. These results depicted that the C-terminal domain in Rv0335c protein facilitated exaggerated apoptotic cell death in THP1 macrophages (Fig. 7c, d).

Role of C-terminal domain of Rv0335c in triggering the activation of Caspases in THP1 macrophages

The activation of initiator Caspase 9 is a pre-requisite for the formation of apoptosome complex and downstream activation of executioner Caspases 3 and 7 which ultimately results in apoptotic cell death. To check the engagement of initiator Caspase 9 with respect to apoptosis induction by our recombinant proteins, western blot analysis of whole cell lysate of 24 h protein-stimulated THP1 macrophages was performed. It was observed that there was prominent activation of Caspase 9 in response to Rv0335c but not in Rv0335cΔCterm protein. The western blot depicted faint band of activated Caspase 9 in Rv0335cΔCterm protein stimulated sample which signifies the role of this C-terminal domain which might facilitate Rv0335c in inducing high levels of Caspase 9 activation (Fig. 8a). Quantification using ImageJ showed that the Rv0335c led to significant levels of activated Caspase9 when compared to unstimulated cells. Rv0335c protein and LPS led to a robust activation of Caspase9 in comparison to Rv0335cΔCterm protein (Fig. 8b).

Following Caspase9 mediated apoptosome formation, Caspase 3 and Caspase 7 are activated as the final executioner Caspases in classical intrinsic apoptosis. As a result, we investigated the role of C-terminal domain of Rv0335c in Caspase 3 and 7 mediated cell death. At all the time points, Rv0335c protein caused significant activation of Caspase 3 and 7 activations in comparison to unstimulated cells. In response to Rv0335cΔCterm protein, we found levels of

Caspase 3 and 7 were comparable to unstimulated cells at 16 and 48 h. There was a significant decrease (~15%) in levels of activated Caspase 3 and 7 in Rv0335cΔCterm-stimulation as compared to Rv0335c-stimulation which was observed at all the time points of study (Fig. 8c and 8d).

To ensure that the apoptosis induction by our recombinant proteins is Caspase-mediated, inhibitor studies were performed using pan caspase inhibitor Z-VAD-fmk. The percentage of Caspase 3 and 7 positive cells was decreased (~1.5-fold) when pre-treated with pan caspase inhibitor Z-VAD-fmk in cells stimulated with Rv0335c/Rv0335cΔCtermproteins and controls at 24 h (Fig. 8e). There was also decrease in percentage of AnnexinV/AnnexinV-PI dual positive cells in Rv0335c/Rv0335cΔCterm-stimulated samples when pre-treated with pan Caspase inhibitor Z-VAD-fmk at 24 h (Fig. 8f). These findings depicts that the putative recombinant proteins cause Caspase-mediated apoptotic cell death in THP1 macrophages.
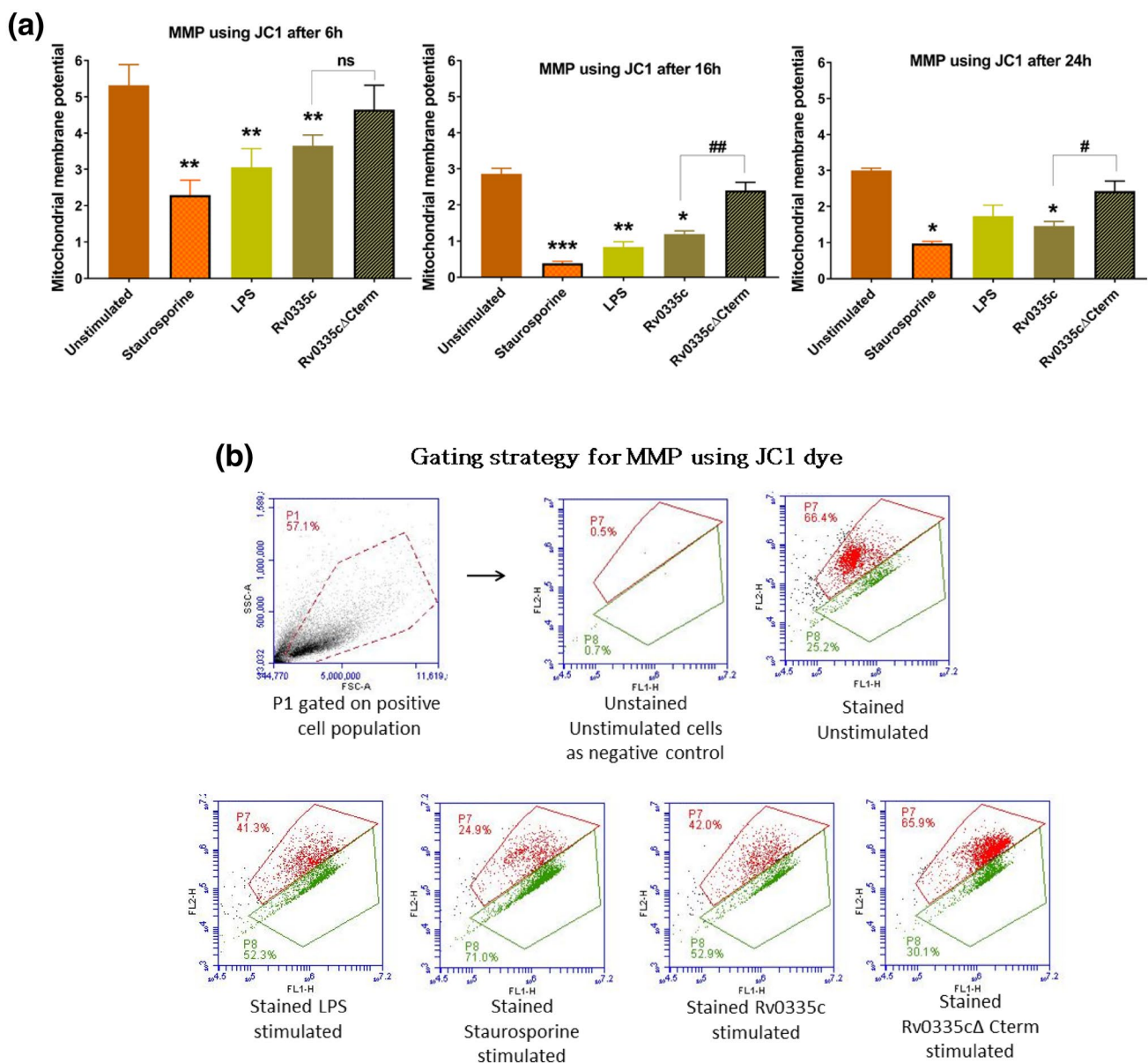
C-terminal domain in Rv0335c protein modulated the host immune response via increased activation of TLR4-HLA-DR-TNF-α signaling cascade

C-terminal domain of Rv0335c facilitated binding of Rv0335c protein with TLR4

Innate immune receptors, particularly TLRs, are crucial determinants in recognition of virulent Mtb proteins. Several PE/PPE proteins have been reported to interact with TLRs. As reported by *Sharma* et al., we also performed initial molecular docking studies and found affinity of Rv0335c to bind TLR4 (data not shown). This is in accordance with reported study on Rv0335c where Rv0335c has been regarded as TLR4 agonist [16]. Docking studies of I-TASSER homology modelled proteins with TLR4 revealed reduced affinity of Rv0335cΔCtermprotein to bind TLR4 than Rv0335c protein (Fig. 9). HADDOCK predicted a score of -120.3 ± -1.5 for Rv0335c-TLR4 docked complex while -92.1 ± -2.8 for Rv0335cΔCterm-TLR4 docked complex. A total of 123 structures clustered into 11 clusters for the TLR4-Rv0335c complex while 79 structures into 8 clusters for the TLR4-Rv0335cΔCterm complex were predicted. The best Z score of -1.9 was predicted for TLR4-Rv0335c complex and -1.1 for TLR4-Rv0335cΔCterm complex. These in silico predictive studies suggested a better interaction of C-terminal domain of Rv0335c with TLR4.

C-terminal domain of Rv0335c protein had role in inducing increased surface expression of TLR4 and antigen presenting HLA-DR molecules

Ca^{2+} binding has also role in stabilizing the TLR-mediated interaction of Mtb proteins [10]. Since, we found an overlap

(a)

(b) Gating strategy for MMP using JC1 dye

Fig. 5 C-terminal domain in Rv0335c had role in inducing host mitochondrial perturbations. THP1 macrophages were left unstimulated or stimulated with controls or recombinant proteins (10 μg/ml) and incubated for varied time points. **a** Mitochondrial Membrane Potential (MMP) was estimated using JC1 dye post 6 h, 16 h and 24 h of stimulation. **b** Gating strategy has been depicted using dot plot where JC1 monomers are represented in green fluorescence and JC1 aggregates are in red. **c** Mitochondrial superoxide levels were estimated following 6 h, 16 h and 24 h of stimulation using MitoSox dye. **d** Histogram depicts the gating strategy where orange fluorescence represents the percentage of Mitochondrial superoxide levels in cells. **e** Release of Cyt C in cell cytosol was assessed with FITC labeled anti-Cyt C antibody. **f** Dot plot represents the gating strategy where percentage of cytoplasmic Cyt C is indicated in red. Graphs were plotted with ratio of ratio of red aggregates/green monomer median fluorescence intensity, % of mitochondrial superoxides or cytoplasmic Cyt C on y axis and control/test protein on x axis. Data was inferred using Student's t test and depicted results are Mean ± SEM of three independent experiments where * represents comparison between control/proteins and unstimulated while # represents comparison between Rv0335c and Rv0335cΔCterm. (#,*) $P < 0.05$, (##,**)$P < 0.01$, (###,***)$P < 0.001$ (Color figure online)

of Ca^{2+} binding residues and C-terminal domain in Rv0335c protein; we were prompted to study the effect of C-terminal domain deletion on expression profile of TLR-HLA-DR and pro-inflammatory cytokines. Surface expression of TLR4 and HLA-DR was estimated by flow cytometry in response to both Rv0335c and Rv0335cΔCterm protein stimulation in THP1 macrophages after 24 h. Rv0335c led to significant increase in surface expression of TLR4 and HLA-DR molecules while Rv0335cΔCterm showed a comparable level of TLR4 and HLA-DR as compared to unstimulated cells.

(c)

(d) Gating strategy for Mitochondrial superoxide using MitoSOX dye
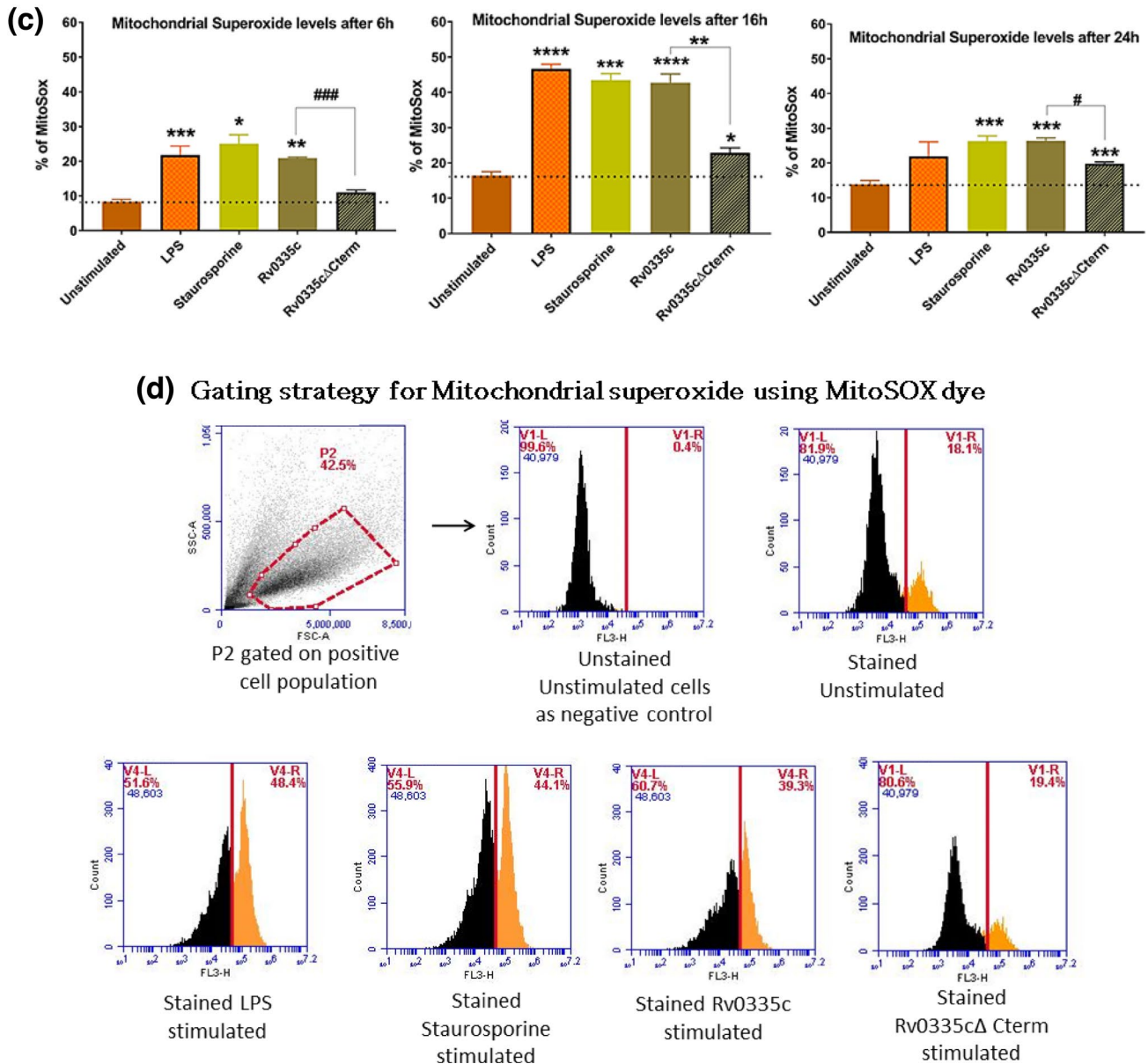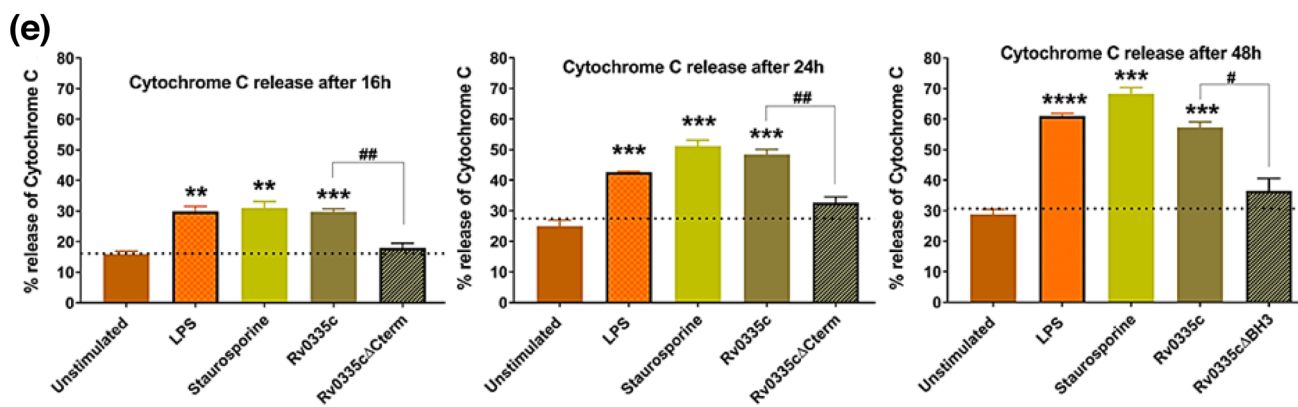

Fig. 5 (continued)

We also observed significant decrease (~ 1.45-fold) in TLR4 and HLA-DR expression in response to Rv0335cΔCterm protein than Rv0335c protein. LPS-a TLR4 agonist resulted in significant increase (~ 1.27-fold) in TLR4 expression while there was no increase of TLR4 expression observed in response to CWF when compared to unstimulated cells. LPS and CWF also showed a significant increased percent positive expression of HLA-DR (~ 1.5-fold) than un-stimulated cells (Fig. 10a–d).

The percentage of TLR4 positive cells reduced considerably when THP1 cells were blocked with Anti-TLR4 antibody prior to stimulation with Rv0335c or controls, implying that Rv0335c function was TLR4 mediated. We examined

HLA-DR levels in cells inhibited with Anti-TLR4 antibody prior to stimulation to determine the role of TLR4-mediated upregulation of Rv0335c-induced HLA-DR expression. In Rv0335c stimulated THP1 macrophages and control cells (LPS and CWF), HLA-DR expression was significantly lower than in unstimulated cells (Fig. 10e, f).

C-terminal domain of Rv0335c led to upregulated levels of pro-inflammatory cytokine TNF-α

Activation of immune response is associated with release of diverse pro-inflammatory cytokines such as TNF-α. Additionally, the various cell death modalities occurring at

(e)

(f) Gating strategy for CytC using FITC labeled Anti-Cytochrome C antibody

P2 gated on positive cell population

Unstained Unstimulated cells as negative control

Stained Unstimulated

Stained LPS stimulated

Stained Staurosporine stimulated

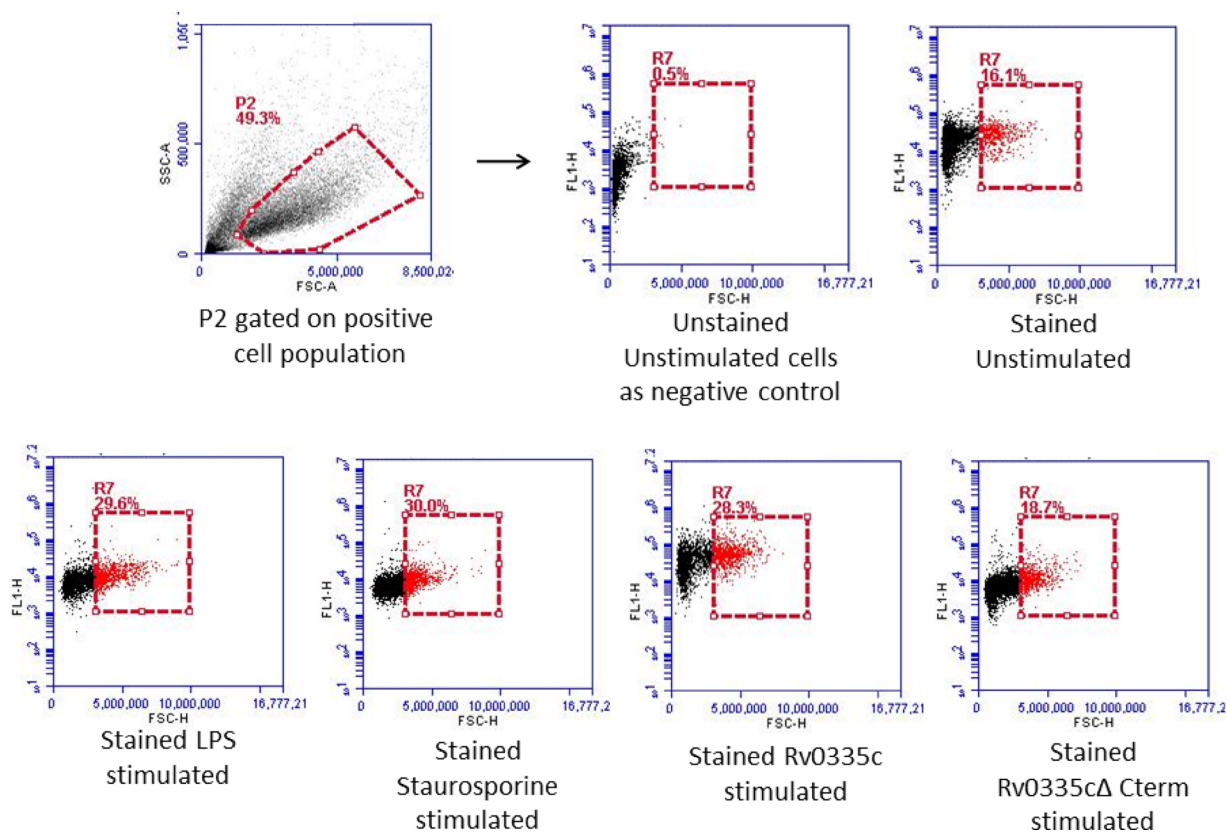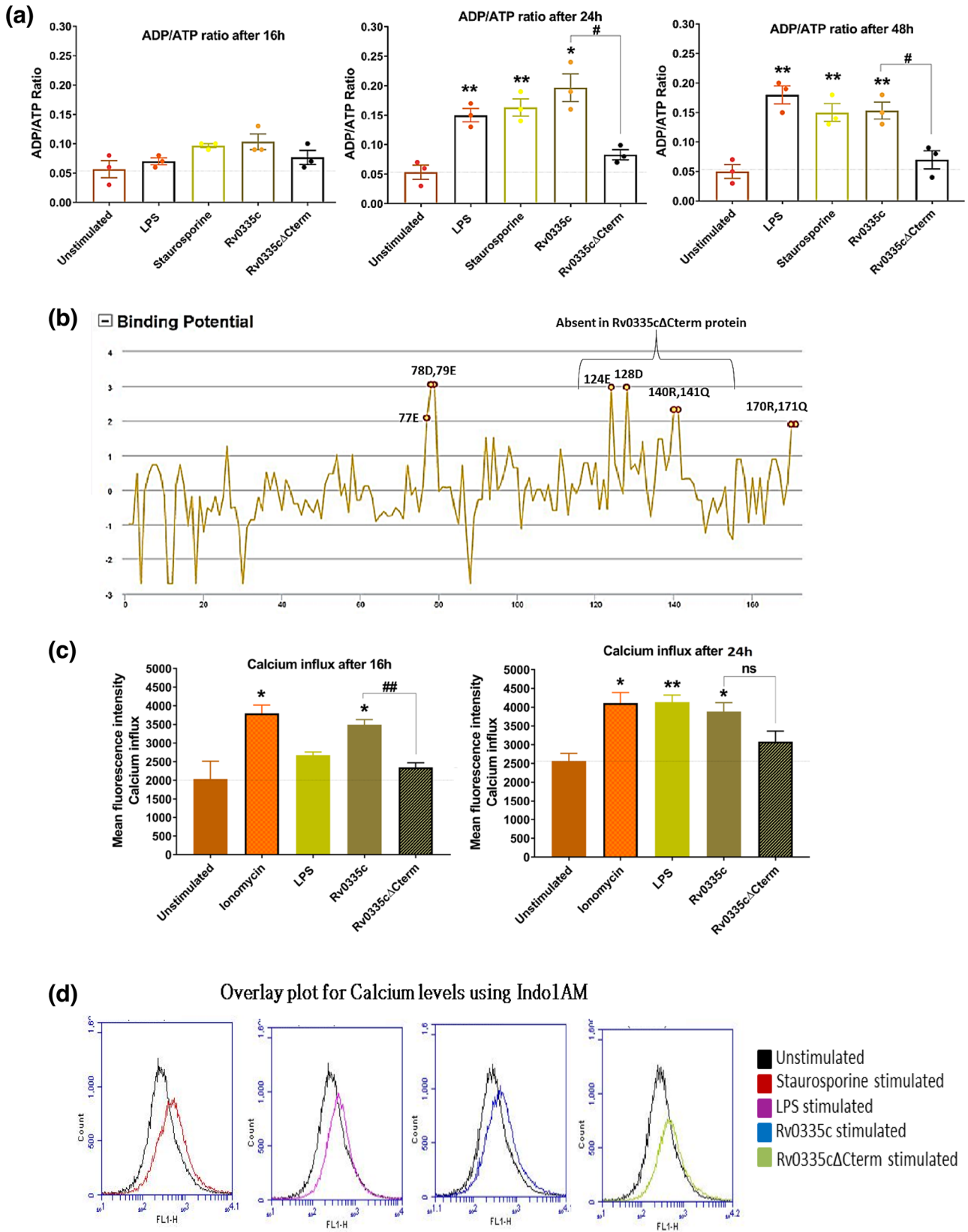Stained Rv0335c stimulated

Stained Rv0335cΔ Cterm stimulated

Fig. 5 (continued)

the host–pathogen interface also involves the expression of TNF-αas pro-inflammatory immune response activation. We found significantly ~ 2.2-fold decreased levels of TNF-α in Rv0335cΔCterm protein in comparison to Rv0335c whole protein at 24 h and 48 h. At 16 h, the levels of TNF-α in Rv0335cΔCterm stimulated cells were comparable to that observed in unstimulated cells. In response to Rv0335c whole protein, we observed significantly increased levels of

TNF-α than unstimulated cells till 48 h of study (Fig. 10g). TLR4 activation has also been linked with activation of another pro-inflammatory cytokine -IL-1β which also additionally activates Caspase 1 mediated inflammasomes activation and Caspase 8 mediated extrinsic apoptosis activation. Interestingly, levels of IL-1β were either comparable to or down-regulated than un-stimulated cells in Rv0335c and Rv0335cΔCterm stimulated macrophages at all the

(a)

ADP/ATP ratio after 16h

ADP/ATP ratio after 24h

ADP/ATP ratio after 48h

(b)

⊟ **Binding Potential**

Absent in Rv0335cΔCterm protein

78D,79E

124E   128D

140R,141Q

77E

170R,171Q

(c)

Calcium influx after 16h

Calcium influx after 24h

(d)

Overlay plot for Calcium levels using Indo1AM

Unstimulated
Staurosporine stimulated
LPS stimulated
Rv0335c stimulated
Rv0335cΔCterm stimulated

◄Fig. 6 C-terminal domain in Rv0335c depleted the intracellular ATP levels and increased the intracellular Ca^{2+} influx. THP1 macrophages were left unstimulated or stimulated with controls or recombinant proteins (10 µg/ml) and incubated for varied time points. **a** ADP/ATP ratio was estimated using plate-based bioluminescence assay. **b** Ca^{2+} binding affinity was predicted for Rv0335c using MIB server. Nine Ca^{2+} binding residues were predicted with four residues in the C-terminal domain of Rv0335c. **c** Ca^{2+} influx was measured by ratio of Mean Fluorescence Intensity (MFI) of 494-nm excitation (bound Ca^{2+}) using flow cytometer. Graphs were plotted with ADP/ATP ratio or MFI of Indo-1AM depicting Ca^{2+} influx on y axis and control/test protein on x axis. Data was inferred using Student's t test and depicted results are Mean ± SEM of three independent experiments where * represents comparison between control/proteins and unstimulated while # represents comparison between Rv0335c and Rv0335cΔCterm. (#,*) $P < 0.05$, (##,**)$P < 0.01$, (###,***)$P < 0.001$. **d** Overlay plot for analysis of Ca^{2+} influx using flow cytometry (Color figure online)

time points (Fig. 10h). IL-1β expression in response to LPS stimulation was found to be significantly 2 to threefold up-regulated than un-stimulated cells till 24 h.

Discussion

Research focused on delineating the molecular function of the PE/PPE proteins has gained a lot of momentum because of their structural uniqueness and co-evolution with virulence-associated ESX system [36, 37]. These proteins have been found to be differentially expressed throughout the varied stages of infection and therefore are speculated to determine the fate of Mtb infection [38, 39].

Rv0335c (PE6) protein of Mtb has recently been implicated to play role in varied host cellular processes such as in upregulation of TLR4-NF-κB-pro-inflammatory canonical cascade, localization within nucleus and mitochondria, potent inducer of caspase-mediated intrinsic apoptosis, suppressor of autophagy, DNA binding and iron acquisition properties. All these findings pointed towards Rv0335c being a significant virulent factor and facilitator of Mtb intracellular survival [16]. Our study further investigated the molecular mechanism behind the apoptosis and mitochondrial stress inducing potential of Rv0335c protein.

We found mitochondrial localization signal sequence in Rv0335c and through a more detailed *in-silico* analysis this protein was also observed to have N terminus TOM20 recognition motif and MPP cleavage site. A thorough sequence scan revealed that the protein was mostly disordered and hydrophobic. Rv0335c was also observed to have two typical BH3-like (L-X-X-X-X-D) motif in which one of these motifs was at the C-terminal of protein. The C-terminal domain in Rv0335c was defined from amino acid position 120 to 166 which was disordered, hydrophobic and contains one BH3-like motif. Multiple sequence alignment pointed out similarities among the C-terminal domain of Rv0335c

and eukaryotic mitochondria-associated pro-apoptotic Bcl2 proteins. The BH3-like motif at the C-terminal domain in Rv0335c was conserved and aligned with the BH3-like motif in pro-apoptotic Bcl2 proteins- Bid and Hrk. Bcl-2 family proteins are the master regulators of apoptosis having at least 18 members, which are divided into three groups based on their role in apoptosis and the number of Bcl-2 homology (BH) domains they have. The Bcl-2 proteins interact with one another through these BH domains forming a complex interaction network to control apoptosis. As a result of their interaction, the fate of cell is determined [17, 40–42]. In addition to the BH-domains, mitochondria-associated Bcl2 proteins also possess a well-characterized C-terminal domain which regulates the apoptogenic function played by these proteins. The C-terminal of these proteins are either hydrophobic or amphipathic, unstructured with abundance of non-polar residues [18]. Therefore, the presence of hydrophobic, disordered C-terminal domain along with BH3-like motif in Rv0335c similar to mitochondria-associated pro-apoptotic Bcl2 proteins suggest the possibility that Rv0335c protein could act as molecular mimic of eukaryotic proteins. Also, Rv0335c may interact via its BH3-like motif to activate the dormant apoptotic Bcl2 proteins to trigger apoptosis. Few studies have shown the molecular mimicry adopted by pathogens including Mtb. The F1L protein of Vaccinia virus possess a BH3-domain which establishes interactions with BH3 peptides of pro-apoptotic proteins such as Bim, Bax and Bak and is a novel example of pathogen adopting molecular mimicry [43]. Two Mtb proteins have also been studied to contain eukaryote-like domains and facilitate infection persistence such as Protein kinase G (PknG) which is a eukaryote-type serine-threonine protein kinase and PE_PGRS29 protein with eukaryote-like ubiquitin-associated (UBA) domain that triggers host xenophagy [12, 44].

To further validate our *in-silico* observations, we performed cloning, expression and purification of Rv0335c protein and Rv0335cΔCterm protein (Rv0335c with deleted C-terminal domain) for experiments with THP1 macrophages as human macrophage model system. Cell viability assay demonstrated significant cell death in response to Rv0335c protein than Rv0335cΔCterm protein suggesting a possible role of C-terminal of Rv0335c in inducing host cell death.

Host mitochondria is a hub of interactions between multiple Bcl-2 proteins. Changes in mitochondrial membrane integrity trigger the activation of pro-apoptotic Bcl2 proteins like Bak and Bax, the release of Cyt C, and the disruption of mitochondrial oxidative phosphorylation, resulting in cellular ATP depletion and the generation of mitochondrial superoxides.[45]. Indeed, the downstream apoptotic pathway involving the activation of the initiator caspase-9 by the apoptotic protease-activating factor-1 requires the release of cytochrome c from the mitochondrial intermembrane space
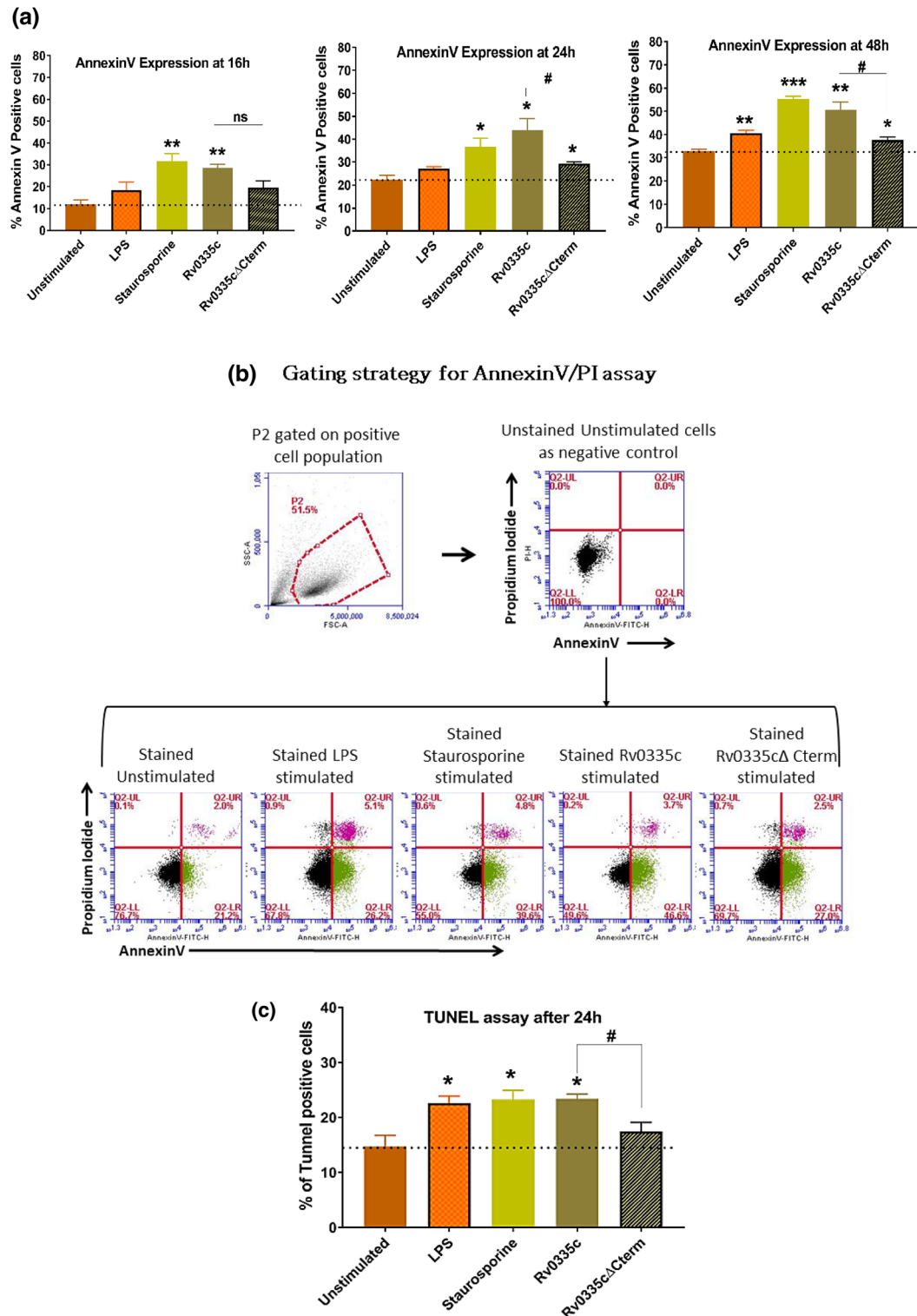
Fig. 7 AnnexinV/PI assay and TUNEL assay to estimate apoptosis in recombinant protein stimulated THP1 macrophages using Flow cytometry. Unstimulated/control/recombinant proteins stimulated THP1 macrophages were incubated for 16 h, 24 h and 48 h. Annexin V-FITC and PI staining of cells was performed followed by acquisition in Flow Cytometer. (a) Time dependent graphs showing percentage of AnnexinV positive cells plotted on y axis and samples on x axis. (b) Gating strategy for analyzing the AnnexinV positive cells where cells in lower right quadrant (green) represents early apoptotic cells, cells in upper right quadrant (pink) represents late apoptotic cells and cells in upper left quadrant represents necrotic cells. c) DNA breaks in response to protein stimulation was estimated with TUNEL assay. d) Gating strategy adopted for TUNEL assay. Data was inferred using Student's t test and depicted results are Mean ± SEM of three independent experiments where * represents comparison between control/proteins and unstimulated while # represents comparison between Rv0335c and Rv0335cΔCterm. (#,*)P < 0.05, (##,**) P < 0.01, (###,***)P < 0.001 (Color figure online)

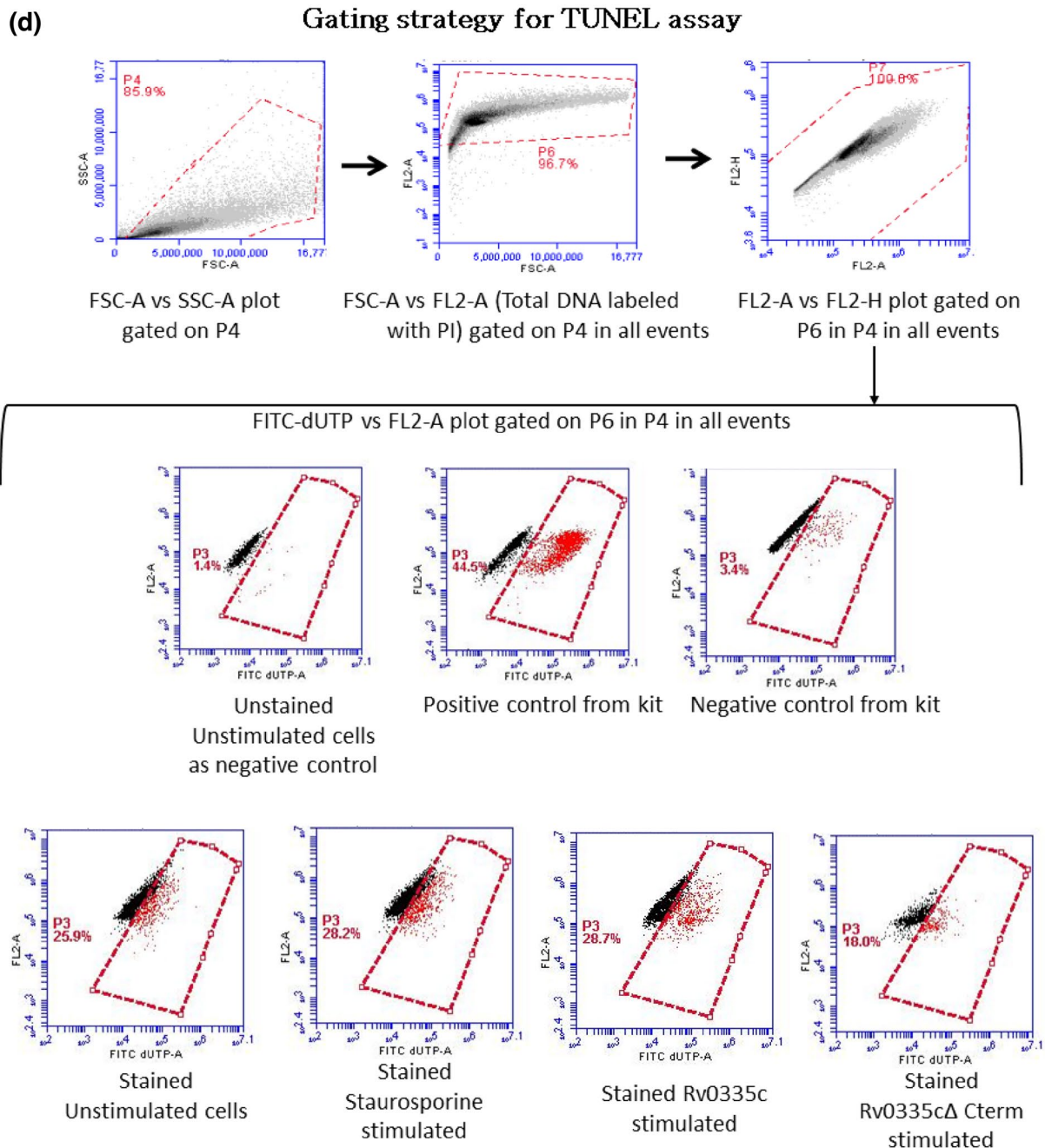**(d) Gating strategy for TUNEL assay**

FSC-A vs SSC-A plot gated on P4

FSC-A vs FL2-A (Total DNA labeled with PI) gated on P4 in all events

FL2-A vs FL2-H plot gated on P6 in P4 in all events

FITC-dUTP vs FL2-A plot gated on P6 in P4 in all events

Unstained Unstimulated cells as negative control

Positive control from kit

Negative control from kit

Stained Unstimulated cells

Stained Staurosporine stimulated

Stained Rv0335c stimulated

Stained Rv0335cΔ Cterm stimulated

Fig. 7 (continued)

[33, 46]. The observations of presence of unique C-terminal domain and BH3-like motif in Rv0335c similar to mitochondria-targeted Bcl2 proteins prompted us to investigate the role of C-terminal domain of Rv0335c protein in causing mitochondrial perturbations. Our results with Rv0335c/Rv0335cΔCterm showed that unlike the whole protein, Rv0335cΔCterm stimulation led to significant reduction in high levels of mitochondrial membrane depolarization, reduction in mitochondrial superoxides levels, reduction in cytoplasmic release of Cyt C and intracellular ATP. Similar observations were reported with other Mtb proteins such as HBHA, Rv1654, Rv0674 and Rv3261c which targeted and disrupted host mitochondrial integrity [47–51]; though the role of C-terminal domain in causing mitochondrial stress have not been investigated. Interestingly, mitochondrial localization studies via confocal microscopy revealed that both Rv0335c and Rv0335cΔCterm proteins were localized to mitochondria of THP1 macrophages. However, difference
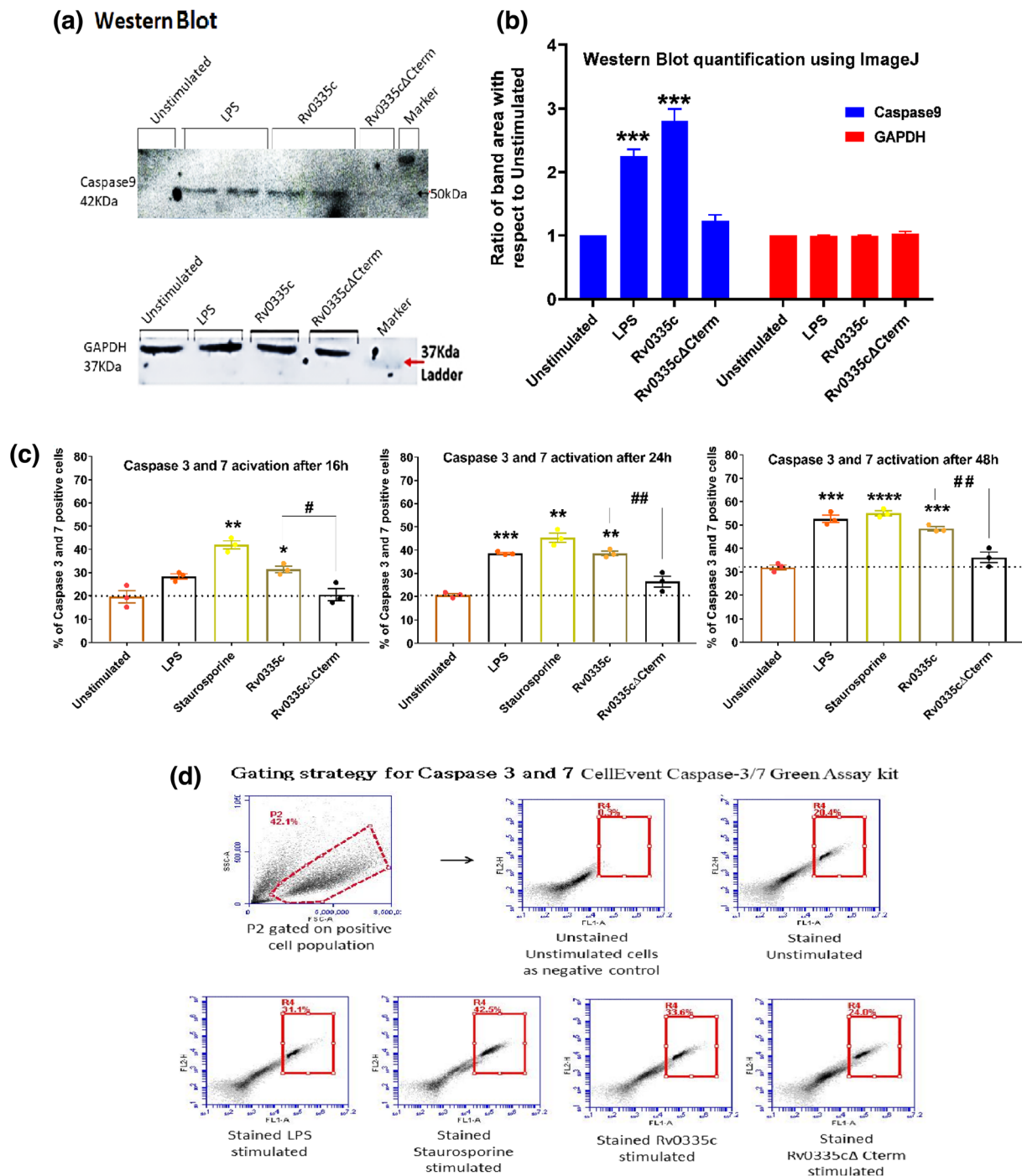
Fig. 8 Estimation of Caspase 9, Caspase 3 and 7 activations in recombinant proteins stimulated THP1 macrophages. **a** Western blot image showing the activation of Caspase9 in THP-1 macrophages left unstimulated or stimulated LPS/Rv2615c protein. Post 24 of stimulation, cell lysate was prepared and fractionated on SDS-PAGE, and proteins were transferred onto the PVDF membrane. Activated Caspase9 levels were estimated using the polyclonal antibody to Caspase9 and an internal loading control GAPDH used at dilution 1:1000. **b** The area of each western blot band was quantified using ImageJ software. Results were analyzed by plotting ratio of each band area with respect to unstimulated cells and are depicted as Mean ± SEM values of three independent experiments. Student's t test was performed where * depicts the comparison with unstimulated cells for each protein separately. **c** Unstimulated/control/recombinant proteins stimulated THP1 macrophages were incubated for different time points (16 h, 24 h and 48 h) and activation of Caspase 3 and 7 was estimated which is a characteristic of intrinsic apoptosis. **d** Gating strategy for Caspase 3 and 7 assay using flow cytometry. THP1 cells were also blocked with z-VAD-fmk Caspase inhibitor prior to stimulation and evaluated for c) levels of Caspases 3 and 7 and d) expression of AnnexinV cell population at 24 h. Data was inferred using Student's t test and depicted results are Mean ± SEM of three independent experiments where * represents comparison between control/proteins and unstimulated while # represents comparison between Rv0335c and Rv0335cΔCterm. (#,*)$P < 0.05$, (##,**) $P < 0.01$, (###,***)$P < 0.001$. (####,****)$P < 0.0001$ (Color figure online)

(e)

(f)
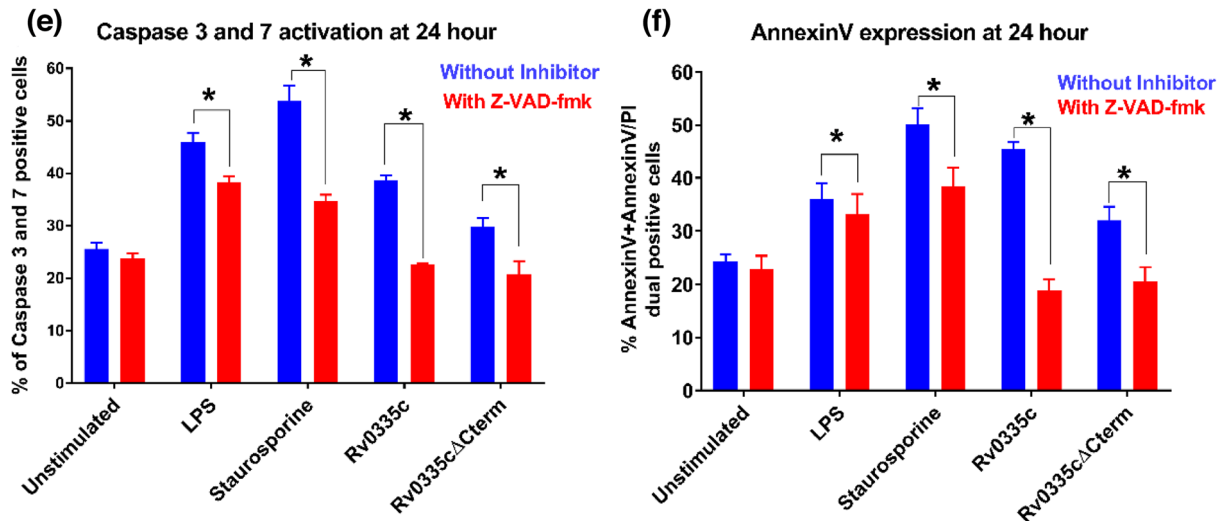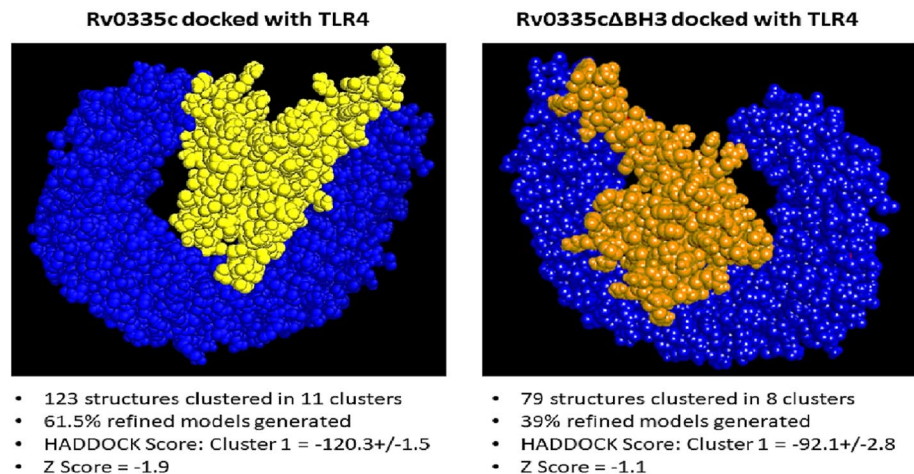

Fig. 9 Molecular docking of Rv0335c/Rv0335cΔCterm proteins with TLR4. HADDOCK server predicted docked complex of Rv0335c (yellow) and Rv0335cΔCterm (orange) bound to TLR4 (blue). The details of each docked complex are enlisted in the figure. The C-terminal domain of Rv0335c protein enhances its binding affinity with TLR4 receptor (Color figure online)

Rv0335c docked with TLR4

- 123 structures clustered in 11 clusters
- 61.5% refined models generated
- HADDOCK Score: Cluster 1 = -120.3+/-1.5
- Z Score = -1.9

Rv0335cΔBH3 docked with TLR4

- 79 structures clustered in 8 clusters
- 39% refined models generated
- HADDOCK Score: Cluster 1 = -92.1+/-2.8
- Z Score = -1.1

in Pearson's coefficient between the intact and C-terminal deleted proteins was observed to be significant, indicating that the C-terminal domain in Rv0335c protein contributes to mitochondrial colocalization, although this does not account for all colocalization. This could be because of intact N terminal mitochondrial localization signal sequence in Rv0335cΔCterm protein similar to Rv0335c protein.

We also observed a time dependent decrease in MitoSpy CMXRos dye intensity indicating a time dependent decrease in mitochondrial membrane potential. This observation of loss of mitochondrial membrane integrity further supported the mitochondrial perturbations induced by Rv0335c protein.

One important aspect which was not discussed in the earlier study on Rv0335c was its ability to disrupt Ca^{2+} homeostasis. Through bio-informatic analysis, we found 9 Ca^{2+} binding residues in Rv0335c protein and 4 of these

residues were found within C-terminal domain in Rv0335c. Our *in-vitro* studies revealed that Rv0335c led to significant increased intracellular Ca^{2+} levels in THP1 macrophages. However, in case of Rv0335cΔCterm protein the effect on Ca^{2+} influx was insignificant. Since Rv0335c protein was observed to target mitochondrial integrity and bioenergetics; its role as modulator of Ca^{2+} signaling seems relevant. Increased intracellular Ca^{2+} levels have been correlated with mitochondrial calcium loading, which result in loss of mitochondrial membrane integrity, release of Cyt c from mitochondria to the cytosol, and ultimately cell death [52]. Furthermore, the PE family proteins have been investigated in terms of establishing a stable Ca^{2+} dependent interaction with TLR [35, 53]; so, it can be inferred that Rv0335c which has been reported to be a TLR4 agonist, binds Ca^{2+} which stabilizes interaction of Rv0335c with TLR4 receptor. An elaborative bio-informatic analysis and experimental
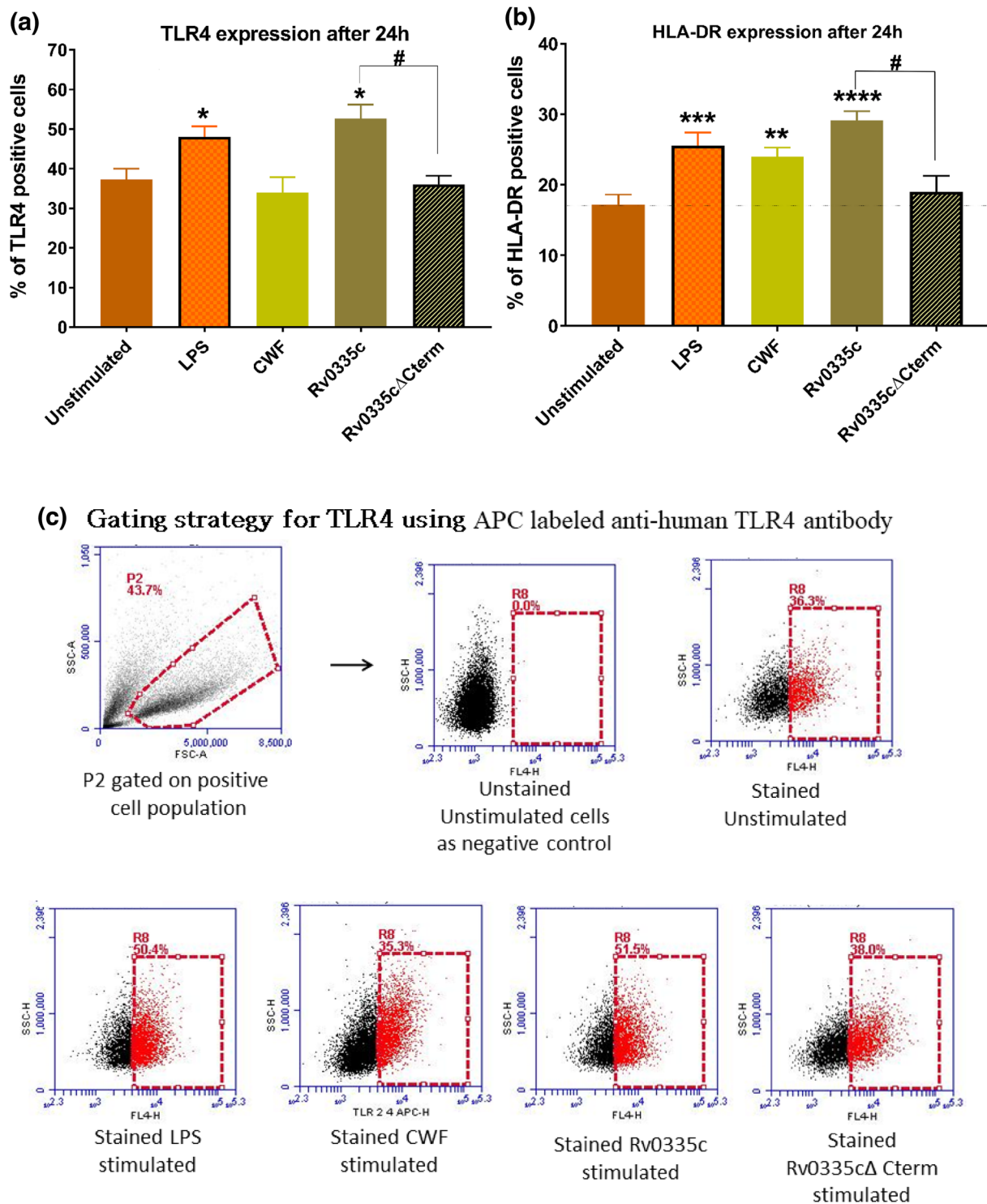
Fig. 10 Expression profile of TLRs, HLA-DR, TNF-α and IL-1β in Rv0335c/Rv0335cΔCterm-stimulated THP1 macrophages. Unstimulated/control/recombinant proteins stimulated THP1 macrophages were incubated for 24 h and expression profile of **a** TLR4, **b** HLA-DR and **g** soluble TNF-α and h) soluble IL-1β were evaluated. THP1 cells were also blocked with Anti-TLR4 antibody prior to stimulation and evaluated for levels of **e** TLR4 and **f** HLA-DR at 24 h. Graphs were plotted for different time points with % of TLR/HLA-DR posi-tive cells or pg/ml of TNF-α/IL-1β on y axis and recombinant pro-teins/control on x axis. Statistical analysis was done with Student's t test and results are Mean ± SEM of three independent experi-ments where * represents comparison between control/proteins and unstimulated while # represents comparison between Rv0335c and Rv0335cΔCterm. (#,*)$P < 0.05$, (##,**)$P < 0.01$, (###,***)$P < 0.001$. (####,****)$P < 0.0001$. Gating strategy adopted for evaluating the surface expression of c) TLR4 and d) HLA-DR (Color figure online)

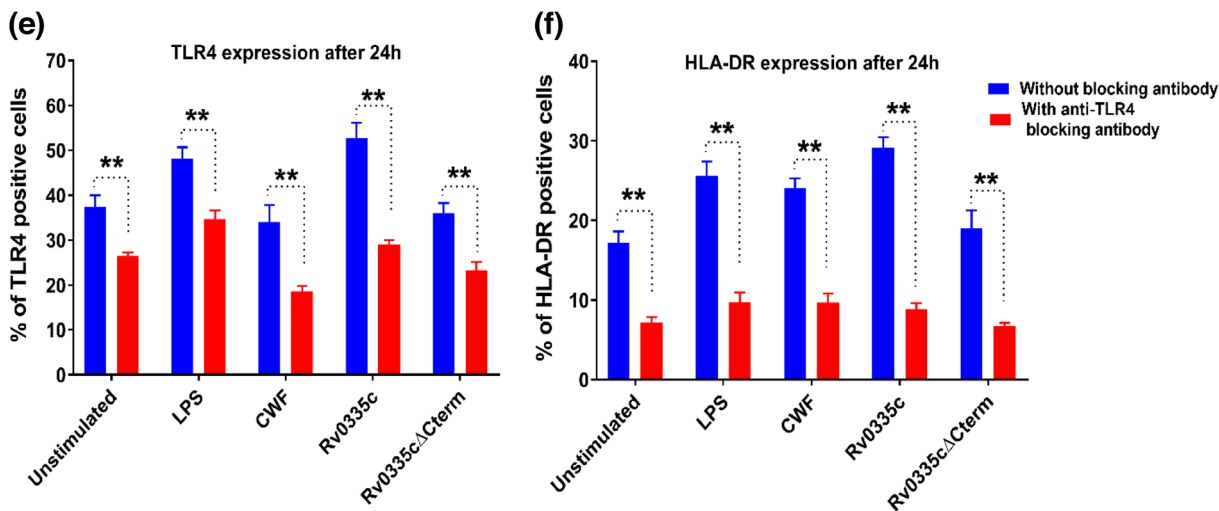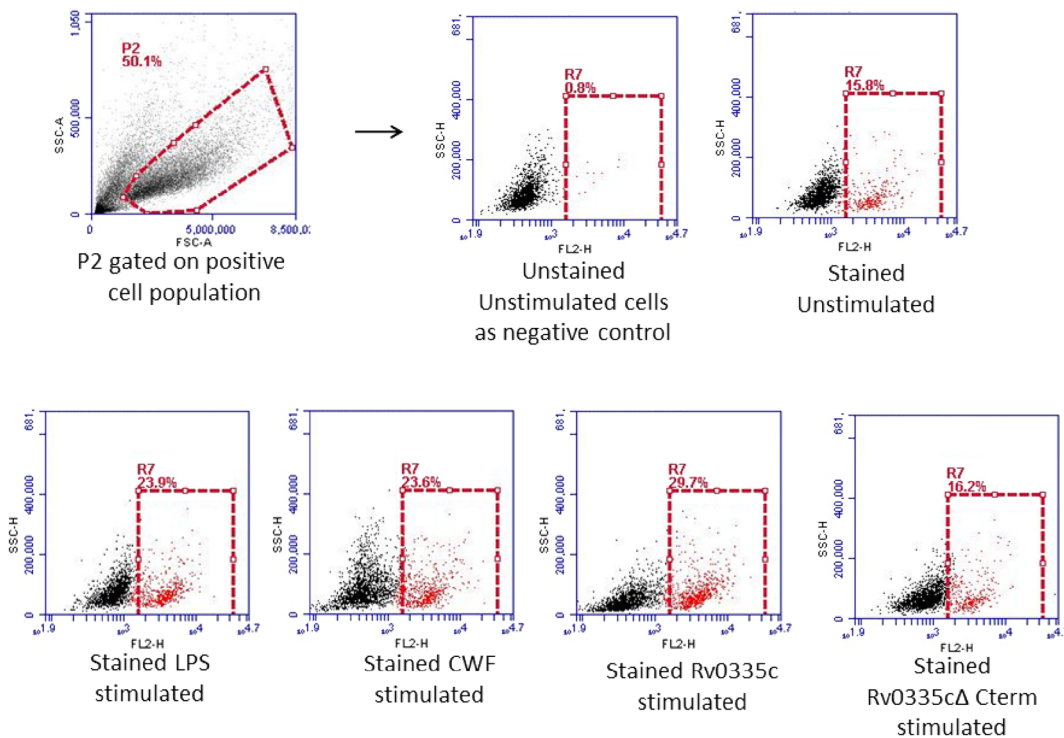**(d)** **Gating strategy for HLA–DR using** PE labeled anti-human HLA-DR antibody

P2 gated on positive cell population

Unstained Unstimulated cells as negative control

Stained Unstimulated

Stained LPS stimulated

Stained CWF stimulated

Stained Rv0335c stimulated

Stained Rv0335cΔ Cterm stimulated

(e) TLR4 expression after 24h

% of TLR4 positive cells

(f) HLA-DR expression after 24h

% of HLA-DR positive cells

Without blocking antibody
With anti-TLR4 blocking antibody

Fig. 10 (continued)

validation has revealed the presence of Ca^{2+} binding motif within several PE_PGRS proteins [34, 35, 53, 54], our study is the first to report the effect of any PE protein on Ca^{2+} homeostasis.

The decision of cell survival or cell death mainly depends on the crucial organelles such as mitochondria which function to maintain cellular homeostasis. Therefore, Mtb proteins targeting mitochondria are important in determining the fate of infection [5]. Since, Rv0335c disrupts host

mitochondrial homeostasis, we probed the role of Rv0335c and the C-terminal domain of Rv0335c in modulating host macrophage apoptosis. Apoptosis detection assays illustrated significant percentage of AnnexinV/AnnexinV-PI dual positive cells, TUNEL positive cells and activated Caspase 9 and executioner Caspases 3 and 7 in response to Rv0335c as compared to Rv0335cΔCterm. This observation signifies the role of C-terminal domain of Rv0335c in inducing apoptosis. Though there has been a lot of debate around the
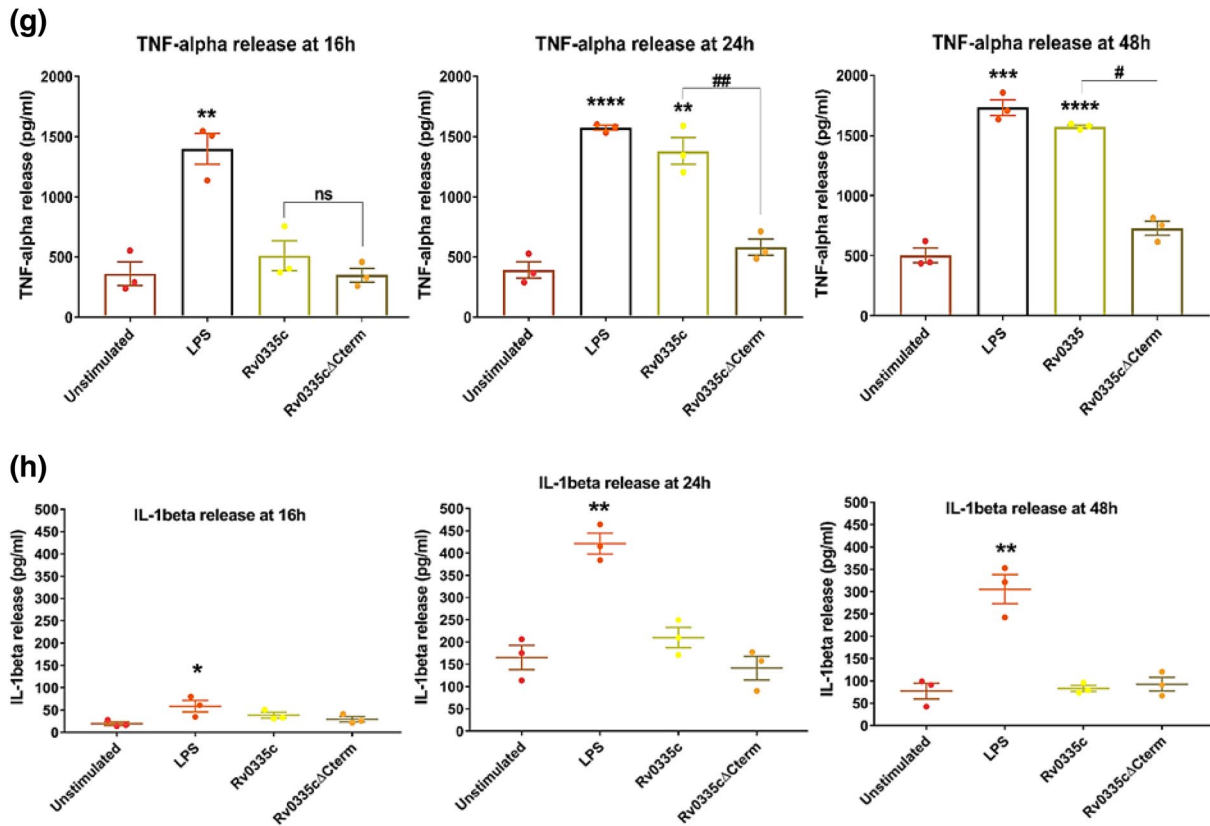
(g)

(h)

Fig. 10 (continued)

implications of cell death modalities during Mtb infection; studies have shown that Mtb harbors both apoptosis inducing and apoptosis inhibiting proteins [55]. Literature suggests that during infection, Mtb favours necrosis which allows for dissemination of pathogen while apoptosis is favoured by the host as defense mechanism to kill the Mtb infected cell [55–61]. Intracellular pathogens like Mtb have evolved strategies to manipulate host cell death to their advantage. Evidences have been presented for both the suppression and activation of apoptosis [62, 63]. Studies have shown that only attenuated Mtb strains promote apoptosis, whereas virulent Mtb strains favour necrotic cell death [64, 65]. Also, there are studies which have shown the apoptosis inducing potential of virulent (H37Rv and Erdman) Mtb strains in host macrophages [66, 67]. Granulomas of the lungs infected with Mtb have shown to include apoptotic macrophages which points toward a positive correlation between apoptosis and pathogen persistence [68, 69]. The members of the ESX-I and ESX-V secretory systems of Mtb have been shown to trigger host cell apoptosis that have implication on pathogen persistence [70–72]. Interestingly, the PE family proteins have co-evolved with the ESX-V secretory system and several PE family proteins such as PE9-PE10, PE_PGRS5, PE_PGRS33 and PE17 have been reported to

induce apoptosis [9, 10, 73–75]. While apoptogenic function played by some of these proteins (PE_PGRS5 and PE17) was confirmed to be beneficial for bacilli survival that may facilitate infection persistence [50, 76]; the apoptosis-inducing potential of others (such as PE9-PE10 and PE_PGRS33) have been discussed to be associated with pathogen survival rather than its killing [9, 73]. Recently in an elaborative review, Mohareer et al., hypothesized that early-stage apoptosis in alveolar macrophages might be a protective pro-host event and late-stage apoptosis at the site of granuloma might be a pro-pathogen process for infection dissemination and persistence [77]. Although, this theory appears convincing; it needs further investigation focused on temporal regulation of apoptosis inducers. Therefore, our study on PE6 corroborates with the study of N. Sharma et al., where PE6 has been reported to be an apoptosis inducing protein and facilitates bacterial survival [16]. Furthermore, our study highlighted the significance of C-terminal domain of Rv0335c protein in inducing macrophage apoptosis and it would be interesting to determine the time of expression of PE6 during the course of infection.

Several proteins in PE family have been reported to engage in host–pathogen interaction via host cell receptors [78, 79]. Rv0335c has been reported to be a TLR4 agonist
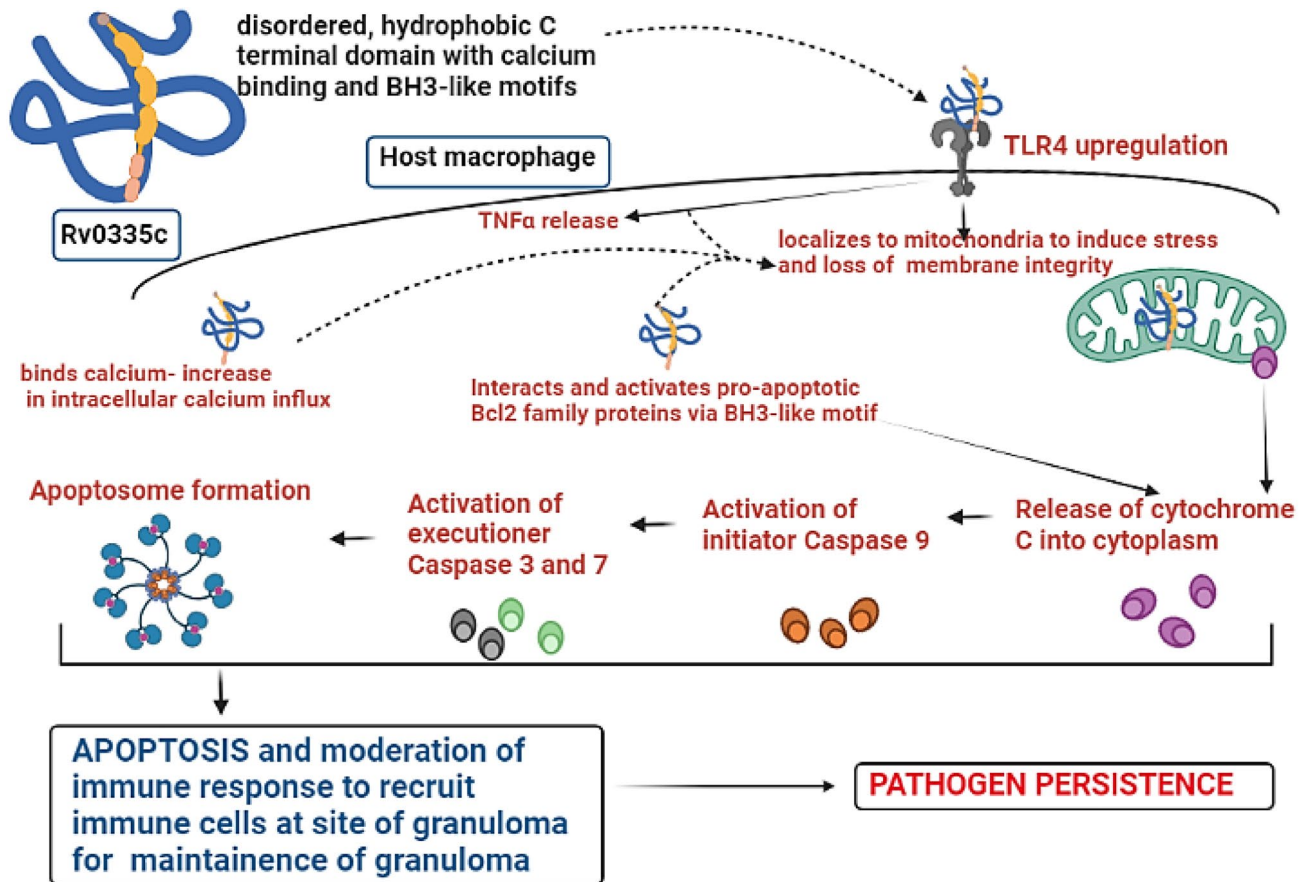
Fig. 11 Mechanism of host cell processes modulation by C-terminal domain of Rv0335c protein of Mtb. Rv0335c protein of Mtb contains N terminal mitochondrial targeting sequence and a unique C-terminal domain and BH3-like motif similar to eukaryotic mitochondrial targeting Bcl2 proteins. Based on our observations of Rv0335c; we hypothesize that the protein activates two parallel host cellular pathways. Through one pathway, the unique C-terminal domain of Rv0335c facilitate its interaction with host TLR4 receptor leading to downstream production of pro-inflammatory cytokine TNF-α. The C-terminal domain of Rv0335c also has role in modulating intracellular Ca^{2+} influx. Through another pathway, Rv0335c localizes to host mitochondria. Because of presence of BH3-like motif in Rv0335c protein, it might be involved in protein–protein interaction

and activation of pro-apoptotic Bcl2 proteins such as Bak, Bax and BH3 only proteins. Activation of Bcl2 proteins through Bak-like BH3 motif containing Rv0335c protein might also trigger the mitochondria mediated intrinsic apoptosis. The C-terminal domain of Rv0335c has role in disruption of mitochondrial integrity in terms of loss of mitochondrial membrane integrity, cytoplasmic release of Cyt C and activation of Caspase 9. Cytoplasmic Cyt C along with Caspase 9 might lead to formation of apoptosome and leads to activation of executioner Caspase 3 and 7. This entire process triggered by Rv0335c protein of Mtb ultimately culminates in host cell apoptosis which may facilitate long term survival of pathogen through cell-to-spread of infection (Color figure online)

which induces the production of pro-inflammatory cytokines like TNF-α [16]. We studied the impact of C-terminal domain of Rv0335c in TLR mediated immune activation and production of pro-inflammatory cytokine. As reported by N. Sharma et al., our molecular docking based *in-silico* results also predicted preferential binding of Rv0335c with TLR4 over TLR2. Interestingly, the deletion of C-terminal domain reduced the binding affinity of Rv0335c protein with TLR4 receptor. To validate the effect of this deletion, *in-vitro* experiments were conducted which revealed that there was no significant upregulation in the surface expression of TLR4-HLA-DR molecules and pro-inflammatory cytokine TNF-α in response to Rv0335cΔCterm protein. Activation

of TLR4 and downstream production of pro-inflammatory cytokines such as TNF-α are pre-requisites for not only activating the host immune response, but also for the development and maintenance of lung granuloma in the late stages of infection [80]. Observation of reduced TLR4-HLA-DR molecules and TNF-α levels in response to Rv0335cΔCterm suggest that the C-terminal domain in Rv0335c aids not only in modulating host mitochondrial functions towards apoptosis, but also in host–pathogen interaction.

Pro-inflammatory cytokine IL-1β is crucial for inflammasome activation and is heterogeneously regulated through TLR4 as well as macrophage metabolic pathways [81]. In our study, we observed insignificant levels of IL-1β in

response to Rv0335c as well as Rv0335cΔCterm recombinant proteins. There are reports that have shown that in persistent Mtb infection, levels of TNF-α are upregulated whereas, glycolytic pathway and IL-1β levels are significantly supressed [82]. Insignificant levels of IL-1β in response to Rv0335c suggest that it acts as a modulator of macrophage functions to ensure pathogen establishment and disease persistence. Our results of high TNF-α and low IL-1β in response to Rv0335c gets support from the study which has reported that Mtb modulate the infected macrophages for its advantage by hijacking the metabolic processes, resolving the exaggerated inflammation and simultaneously keeping the macrophages active to allow bacilli replication and persistence [83].

Conclusively, the presence of eukaryote-like C-terminal domain and BH3-like motif in Rv0335c could be a phenomenon of molecular mimicry adopted by Mtb to circumvent the host cell responses towards programmed cell death or apoptosis. Additionally, the modulation of various host cell processes such mitochondrial integrity, Ca^{2+} homeostasis and TLR4-mediated cytokine release by a single Mtb protein Rv0335c enhances our understanding of Mtb pathogenesis (Fig. 11). The role of this protein in facilitating pathogen persistence and as promising therapeutic target for TB needs further investigations.

Author contributions MS and M: contributed equally in conceptualization, methodology and writing of the manuscript. M and P: conducted all the experiments. PB: performed the cloning, expression and purification of Rv0335c protein. MS and SS contributed in reviewing and editing of the manuscript.

Data availability All data generated or analyzed during this study are included in this published article (and its supplementary information files). Extensive datasets related to the study can be provided by the corresponding author and can be provided upon request.

Declarations

Conflict of interest The authors have no competing interests to declare.

References

1. WHO (2021) WHO global TB report. World Health Organization, Geneva
2. Issar S (2003) *Mycobacterium tuberculosis* pathogenesis and molecular determinants of virulence. Clin Microbiol Rev 16:463–496. https://doi.org/10.1128/CMR.16.3.463-496.2003
3. Prozorov AA, Fedorova IA, Bekker OB, Danilenko VN (2014) The virulence factors of *Mycobacterium tuberculosis*: genetic control, new conceptions. Russ J Genet 50:775–797. https://doi.org/10.1134/S1022795414080055
4. Chai Q, Wang L, Liu CH (2020) New insights into the evasion of host innate immunity by *Mycobacterium tuberculosis*. Cell Mol Immunol. https://doi.org/10.1038/s41423-020-0502-z
5. Dubey RK (2016) Assuming the role of mitochondria in mycobacterial infection. Int J Mycobacteriol 5:379–383. https://doi.org/10.1016/j.ijmyco.2016.06.001
6. McGuire AM, Weiner B, Park ST et al (2012) Comparative analysis of mycobacterium and related actinomycetes yields insight into the evolution of mycobacterium tuberculosis pathogenesis. BMC Genomics. https://doi.org/10.1186/1471-2164-13-120
7. Singh PP, Parra M, Cadieux N, Brennan MJ (2008) A comparative study of host response to three *Mycobacterium tuberculosis* PE_PGRS proteins. Microbiology 154:3469–3479. https://doi.org/10.1099/mic.0.2008/019968-0
8. Chaturvedi R, Bansal K, Narayana Y et al (2010) The multifunctional PE-PGRS11 protein from *Mycobacterium tuberculosis* plays a role in regulating resistance to oxidative stress. J Biol Chem 285:30389–30403. https://doi.org/10.1074/jbc.M110.135251
9. Tiwari B, Ramakrishnan UM, Raghunand TR (2015) The *Mycobacterium tuberculosis* protein pair PE9 (Rv1088)–PE10 (Rv1089) forms heterodimers and induces macrophage apoptosis through toll-like receptor 4. Cell Microbiol 17:1653–1669. https://doi.org/10.1111/cmi.12462
10. Grover S, Sharma T, Singh Y et al (2018) The PGRS domain of *Mycobacterium tuberculosis* PE_PGRS protein Rv0297 is involved in endoplasmic reticulum stress-mediated apoptosis through toll-like receptor 4. MBio. https://doi.org/10.1128/mBio.01017-18
11. Augenstreich J, Arbues A, Simeone R et al (2017) ESX-1 and phthiocerol dimycocerosates of *Mycobacterium tuberculosis* act in concert to cause phagosomal rupture and host cell apoptosis. Cell Microbiol 19:e12726. https://doi.org/10.1111/cmi.12726
12. Chai Q, Wang X, Qiang L et al (2019) A *Mycobacterium tuberculosis* surface protein recruits ubiquitin to trigger host xenophagy. Nat Commun 10:1973. https://doi.org/10.1038/s41467-019-09955-8
13. Faridgohar M, Nikoueinejad H (2017) New findings of toll-like receptors involved in *Mycobacterium tuberculosis* infection. Pathog Glob Health 111:256–264
14. Harding CV, Boom WH (2010) Regulation of antigen presentation by *Mycobacterium tuberculosis*: a role for toll-like receptors. Nat Rev Microbiol 8:296–307. https://doi.org/10.1038/nrmicro2321
15. Stamm CE, Collins AC, Shiloh MU (2015) Sensing of M ycobacterium tuberculosis and consequences to both host and bacillus. Immunol Rev 264:204–219
16. Sharma N, Shariq M, Quadir N et al (2021) *Mycobacterium tuberculosis* protein PE6 (Rv0335c), a novel TLR4 agonist, evokes an inflammatory response and modulates the cell death pathways in macrophages to enhance intracellular survival. Front Immunol 12:696491. https://doi.org/10.3389/fimmu.2021.696491

17. Shamas-Din A, Brahmbhatt H, Leber B, Andrews DW (2011) BH3-only proteins: orchestrators of apoptosis. Biochim Biophys Acta - Mol Cell Res 1813:508–520. https://doi.org/10.1016/j.bbamcr.2010.11.024

18. Gómez-Fernández JC (2014) Functions of the C-terminal domains of apoptosis-related proteins of the Bcl-2 family. Chem Phys Lipids 183:77–90. https://doi.org/10.1016/j.chemphyslip.2014.05.003

19. O'Brien MA, Kirby R (2008) Apoptosis: a review of pro-apoptotic and anti-apoptotic pathways and dysregulation in disease. J Vet Emerg Crit Care 18:572–585. https://doi.org/10.1111/j.1476-4431.2008.00363.x

20. Lomonosova E, Chinnadurai G (2008) BH3-only proteins in apoptosis and beyond: an overview. Oncogene 27(Suppl 1):S2–S19. https://doi.org/10.1038/onc.2009.39

21. Pierleoni A, Martelli PL, Casadio R (2011) MemLoci: predicting subcellular localization of membrane proteins in eukaryotes. Bioinformatics 27:1224–1230. https://doi.org/10.1093/bioinformatics/btr108

22. Fukasawa Y, Tsuji J, Fu S-C et al (2015) MitoFates: improved prediction of mitochondrial targeting sequences and their cleavage sites*. Mol Cell Proteomics 14:1113–1126. https://doi.org/10.1074/mcp.M114.043083

23. Dunker AK, Brown CJ, Lawson JD et al (2002) Intrinsic disorder and protein function. Biochemistry 41:6573–6582. https://doi.org/10.1021/bi012159+

24. Dunker AK, Lawson JD, Brown CJ et al (2001) Intrinsically disordered protein. J Mol Graph Model 19:26–59. https://doi.org/10.1016/S1093-3263(00)00138-8

25. Cao B, Porollo A, Adamczak R et al (2006) Enhanced recognition of protein transmembrane domains with prediction-based structural profiles. Bioinformatics 22:303–309. https://doi.org/10.1093/bioinformatics/bti784

26. Roy A, Kucukural A, Zhang Y (2010) I-TASSER: a unified platform for automated protein structure and function prediction. Nat Protoc 5:725–738. https://doi.org/10.1038/nprot.2010.5

27. Yang J, Zhang Y (2015) I-TASSER server: new development for protein structure and function predictions. Nucleic Acids Res 43:W174–W181. https://doi.org/10.1093/nar/gkv342

28. Ramachandran S, Kota P, Ding F, Dokholyan NV (2011) Automated minimization of steric clashes in protein structures. Proteins 79:261–270. https://doi.org/10.1002/prot.22879

29. Colovos C, Yeates TO (1993) Verification of protein structures: patterns of nonbonded atomic interactions. Protein Sci 2:1511–1519. https://doi.org/10.1002/pro.5560020916

30. Bowie JU, Lüthy R, Eisenberg D (1991) A method to identify protein sequences that fold into a known three-dimensional structure. Science 253:164–170. https://doi.org/10.1126/science.1853201

31. Laskowski RA, Rullmannn JA, MacArthur MW et al (1996) AQUA and PROCHECK-NMR: programs for checking the quality of protein structures solved by NMR. J Biomol NMR 8:477–486. https://doi.org/10.1007/BF00228148

32. Lin Y-F, Cheng C-W, Shih C-S et al (2016) MIB: metal ion-binding site prediction and docking serveR. J Chem Inf Model 56:2287–2291. https://doi.org/10.1021/acs.jcim.6b00407

33. Giam M, Huang DCS, Bouillet P (2008) BH3-only proteins and their roles in programmed cell death. Oncogene 27:S128–S136. https://doi.org/10.1038/onc.2009.50

34. Bachhawat N, Singh B (2007) Mycobacterial PE-PGRS proteins contain calcium-binding motifs with parallel β-roll folds. Genomics Proteomics Bioinform 5:236–241. https://doi.org/10.1016/S1672-0229(08)60010-8

35. Yeruva VC, Kulkarni A, Khandelwal R et al (2016) The PE_PGRS proteins of *Mycobacterium tuberculosis* Are Ca2+ binding mediators of host-pathogen interaction. Biochemistry 55:4675–4687. https://doi.org/10.1021/acs.biochem.6b00289

36. Fishbein S, van Wyk N, Warren RM, Sampson SL (2015) Phylogeny to function: PE/PPE protein evolution and impact on *Mycobacterium tuberculosis* pathogenicity. Mol Microbiol 96:901–916. https://doi.org/10.1111/mmi.12981

37. Ates LS (2020) New insights into the mycobacterial PE and PPE proteins provide a framework for future research. Mol Microbiol 113:4–21. https://doi.org/10.1111/mmi.14409

38. Voskuil MI, Schnappinger D, Rutherford R et al (2004) Regulation of the *Mycobacterium tuberculosis* PE/PPE genes. Tuberculosis 84:256–262. https://doi.org/10.1016/j.tube.2003.12.014

39. Sampson SL (2011) Mycobacterial PE/PPE proteins at the host-pathogen interface. Clin Dev Immunol 2011:497203. https://doi.org/10.1155/2011/497203

40. Chipuk JE, Moldoveanu T, Llambi F et al (2010) The BCL-2 family reunion. Mol Cell 37:299–310

41. Dewson G, Kratina T, Sim HW et al (2008) To trigger apoptosis, Bak exposes its BH3 domain and homodimerizes via BH3: groove interactions. Mol Cell 30:369–380. https://doi.org/10.1016/j.molcel.2008.04.005

42. Dewson G, Ma S, Frederick P et al (2012) Bax dimerizes via a symmetric BH3: groove interface during apoptosis. Cell Death Differ 19:661–670

43. Kvansakul M, Yang H, Fairlie WD et al (2008) Vaccinia virus anti-apoptotic F1L is a novel Bcl-2-like domain-swapped dimer that binds a highly selective subset of BH3-containing death ligands. Cell Death Differ 15:1564–1571. https://doi.org/10.1038/cdd.2008.83

44. Wang J, Ge P, Lei Z et al (2021) *Mycobacterium tuberculosis* protein kinase G acts as an unusual ubiquitinating enzyme to impair host immunity. EMBO Rep 22:e52175. https://doi.org/10.15252/embr.202052175

45. Peña-Blanco A, García-Sáez AJ (2018) Bax, Bak and beyond — mitochondrial performance in apoptosis. FEBS J 285:416–431. https://doi.org/10.1111/febs.14186

46. Cory S, Adams JM (2002) The Bcl2 family: regulators of the cellular life-or-death switch. Nat Rev Cancer 2:647–656

47. Sohn H, Kim J-S, Shin SJ et al (2011) Targeting of *Mycobacterium tuberculosis* heparin-binding hemagglutinin to mitochondria in macrophages. PLOS Pathog 7:e1002435

48. Choi J-A, Lim Y-J, Cho S-N et al (2013) Mycobacterial HBHA induces endoplasmic reticulum stress-mediated apoptosis through the generation of reactive oxygen species and cytosolic Ca2+ in murine macrophage RAW 264.7 cells. Cell Death Dis 4:e957. https://doi.org/10.1038/cddis.2013.489

49. Lee K-I, Choi S, Choi H-G et al (2020) Recombinant Rv3261 protein of *Mycobacterium tuberculosis* induces apoptosis through a mitochondrion-dependent pathway in macrophages and inhibits intracellular bacterial growth. Cell Immunol 354:104145. https://doi.org/10.1016/j.cellimm.2020.104145

50. Lee K-I, Choi S, Choi H-G et al (2021) Recombinant Rv1654 protein of *Mycobacterium tuberculosis* induces mitochondria-mediated apoptosis in macrophage. Microbiol Immunol 65:178–188. https://doi.org/10.1111/1348-0421.12880

51. Dubey RK, Dhamija E, Kumar Mishra A et al (2021) Mycobacterial origin protein Rv0674 localizes into mitochondria, interacts with D-loop and regulates OXPHOS for intracellular persistence of *Mycobacterium tuberculosis*. Mitochondrion 57:241–256. https://doi.org/10.1016/j.mito.2020.11.014

52. Rizzuto R, De Stefani D, Raffaello A, Mammucari C (2012) Mitochondria as sensors and regulators of calcium signalling. Nat Rev Mol Cell Biol 13:566–578. https://doi.org/10.1038/nrm3412

53. Sharma T, Singh J, Grover S et al (2021) PGRS domain of Rv0297 of *Mycobacterium tuberculosis* functions in a calcium dependent manner. Int J Mol Sci 22:9390

54. Meena LS (2019) Interrelation of Ca(2+) and PE_PGRS proteins during *Mycobacterium tuberculosis* pathogenesis. J Biosci 44:1–7

55. Behar SM, Martin CJ, Booty MG et al (2011) Apoptosis is an innate defense function of macrophages against *Mycobacterium tuberculosis*. Mucosal Immunol 4:279–287. https://doi.org/10.1038/mi.2011.3

56. Dobos KM, Spotts EA, Quinn FD, King CH (2000) Necrosis of lung epithelial cells during infection with *Mycobacterium tuberculosis* is preceded by cell permeation. Infect Immun 68:6300–6310. https://doi.org/10.1128/IAI.68.11.6300-6310.2000

57. Gil DP, León LG, Correa LI et al (2004) Differential induction of apoptosis and necrosis in monocytes from patients with tuberculosis and healthy control subjects. J Infect Dis 189:2120–2128. https://doi.org/10.1086/386369

58. Saunders BM, Britton WJ (2007) Life and death in the granuloma: immunopathology of tuberculosis. Immunol Cell Biol 85:103–111. https://doi.org/10.1038/sj.icb.7100027

59. Moraco AH, Kornfeld H (2014) Cell death and autophagy in tuberculosis. Semin Immunol 26:497–511. https://doi.org/10.1016/j.smim.2014.10.001

60. Stutz MD, Allison CC, Ojaimi S et al (2021) Macrophage and neutrophil death programs differentially confer resistance to tuberculosis. Immunity 54:1758-1771.e7. https://doi.org/10.1016/j.immuni.2021.06.009

61. Arnett E, Schlesinger LS (2021) Live and let die: TB control by enhancing apoptosis. Immunity 54:1625–1627. https://doi.org/10.1016/j.immuni.2021.07.010

62. Divangahi M, Chen M, Gan H et al (2009) *Mycobacterium tuberculosis* evades macrophage defenses by inhibiting plasma membrane repair. Nat Immunol 10:899–906

63. Aporta A, Arbues A, Aguilo JI et al (2012) Attenuated *Mycobacterium tuberculosis* SO2 vaccine candidate is unable to induce cell death. PLoS ONE. https://doi.org/10.1371/journal.pone.0045213

64. Gräb J, Suárez I, van Gumpel E et al (2019) Corticosteroids inhibit *Mycobacterium tuberculosis*-induced necrotic host cell death by abrogating mitochondrial membrane permeability transition. Nat Commun 10:688. https://doi.org/10.1038/s41467-019-08405-9

65. Zhao X, Khan N, Gan H et al (2017) Bcl-xL mediates RIPK3-dependent necrosis in M. tuberculosis-infected macrophages. Mucosal Immunol 10:1553–1568

66. Schaible UE, Winau F, Sieling PA et al (2003) Apoptosis facilitates antigen presentation to T lymphocytes through MHC-I and CD1 in tuberculosis. Nat Med 9:1039–1046. https://doi.org/10.1038/nm906

67. Danelishvili L, McGarvey J, Li Y-J, Bermudez LE (2003) *Mycobacterium tuberculosis* infection causes different levels of apoptosis and necrosis in human macrophages and alveolar epithelial cells. Cell Microbiol 5:649–660. https://doi.org/10.1046/j.1462-5822.2003.00312.x

68. Fayyazi A, Eichmeyer B, Soruri A et al (2000) Apoptosis of macrophages and T cells in tuberculosis associated caseous necrosis. J Pathol 191:417–425

69. Pan H, Yan B-S, Rojas M et al (2005) Ipr1 gene mediates innate immunity to tuberculosis. Nature 434:767–772

70. Davis JM, Ramakrishnan L (2009) The role of the granuloma in expansion and dissemination of early tuberculous infection. Cell 136:37–49

71. Abdallah AM, Bestebroer J, Savage NDL et al (2011) Mycobacterial secretion systems ESX-1 and ESX-5 Play distinct roles in host cell death and inflammasome activation. J Immunol 187:4744–4753. https://doi.org/10.4049/jimmunol.1101457

72. Aguilo JI, Alonso H, Uranga S et al (2013) ESX-1-induced apoptosis is involved in cell-to-cell spread of *Mycobacterium tuberculosis*. Cell Microbiol 15:1994–2005. https://doi.org/10.1111/cmi.12169

73. Basu S, Pathak SKS, Banerjee A et al (2007) Execution of macrophage apoptosis by PE_PGRS33 of *Mycobacterium tuberculosis* is mediated by toll-like receptor 2-dependent release of tumor necrosis factor-α. J Biol Chem 282:1039–1050. https://doi.org/10.1074/jbc.M604379200

74. Cadieux N, Parra M, Cohen H et al (2011) Induction of cell death after localization to the host cell mitochondria by the *Mycobacterium tuberculosis* PE_PGRS33 protein. Microbiology 157:793–804. https://doi.org/10.1099/mic.0.041996-0

75. Abo-Kadoum MA, Assad M, Ali MK et al (2021) *Mycobacterium tuberculosis* PE17 (Rv1646) promotes host cell apoptosis via host chromatin remodeling mediated by reduced H3K9me3 occupancy. Microb Pathog 159:105147. https://doi.org/10.1016/j.micpath.2021.105147

76. Sharma T, Grover S, Arora N et al (2020) PGRS Domain of Rv0297 of *Mycobacterium tuberculosis* Is Involved in Modulation of Macrophage Functions to Favor Bacterial Persistence. Front Cell Infect Microbiol. https://doi.org/10.3389/fcimb.2020.00451

77. Mohareer K, Medikonda J, Vadankula GR (2020) Mycobacterial control of host mitochondria: bioenergetic and metabolic changes shaping cell fate and infection outcome. Front Cell Infect Microbiol. https://doi.org/10.3389/fcimb.2020.00457

78. Ortega-Tirado D, Niño-Padilla EI, Arvizu-Flores AA et al (2020) Identification of immunogenic T-cell peptides of *Mycobacterium tuberculosis* PE_PGRS33 protein. Mol Immunol 125:123–130. https://doi.org/10.1016/j.molimm.2020.06.026

79. Medha P, Sharma S, Sharma M (2022) Design of a peptide-based vaccine from late stage specific immunogenic cross-reactive antigens of PE/PPE proteins of *Mycobacterium tuberculosis*. Eur J Pharm Sci Off J Eur Fed Pharm Sci 168:106051. https://doi.org/10.1016/j.ejps.2021.106051

80. Dorhoi A, Kaufmann SHE (2014) Tumor necrosis factor alpha in mycobacterial infection. Semin Immunol 26:203–209. https://doi.org/10.1016/j.smim.2014.04.003

81. Gleeson LE, Sheedy FJ, Palsson-McDermott EM et al (2016) Cutting edge: *Mycobacterium tuberculosis* induces aerobic glycolysis in human alveolar macrophages that is required for control of intracellular bacillary replication. J Immunol 196:2444–2449. https://doi.org/10.4049/jimmunol.1501612

82. Próchnicki T, Latz E (2017) Inflammasomes on the crossroads of innate immune recognition and metabolic control. Cell Metab 26:71–93. https://doi.org/10.1016/j.cmet.2017.06.018

83. Das A, Ganesh K, Khanna S et al (2014) Engulfment of apoptotic cells by macrophages: a role of MicroRNA-21 in the resolution of wound inflammation. J Immunol 192:1120–1129. https://doi.org/10.4049/jimmunol.1300613